


OsHIPL1, a hedgehog-interacting protein-like 1 protein, increases seed vigour in rice

Ying He, Shanshan Chen, Kexin Liu, Yongji Chen, Yanhao Cheng, Peng Zeng, Peiwen Zhu, Ting Xie, Sunlu Chen, Hongsheng Zhang* and Jinping Cheng* 

State Key Laboratory of Crop Genetics and Germplasm Enhancement, Jiangsu Collaborative Innovation Center for Modern Crop Production, Jiangsu Province Engineering Research Center of Seed Industry Science and Technology, Cyrus Tang Innovation Center for Seed Industry, Nanjing Agricultural University, Nanjing, China

Received 27 December 2021;

revised 19 February 2022;

accepted 9 March 2022.

*Correspondence (Tel 86-02-584396075;

fax 86-02-584396075;

email cjp@njau.edu.cn (J.C.); Tel 86-02-

584396075; fax 86-02-584396075;

email hszhang@njau.edu.cn (H.Z.)

Summary

The cultivation of rice varieties with high seed vigour is vital for the direct seeding of rice, and the molecular basis of regulation of seed vigour remains elusive. Here, we cloned a new gene *OsHIPL1*, which encodes hedgehog-interacting protein-like 1 protein as a causal gene of the major QTL *qSV3* for rice seed vigour. *OsHIPL1* was mainly localized in the plasma membrane and nucleus. RNA sequencing (RNA-seq) revealed that the ABA-related genes were involved in the *OsHIPL1* regulation of seed vigour in rice. The higher levels of endogenous ABA were measured in germinating seeds of *OsHIPL1* mutants and NIL-*qsv3* line compared to IR26 plants, with two up-regulated ABA biosynthesis genes (*OsZEP* and *OsNCED4*) and one down-regulated ABA catabolism gene *OsABA8ox3*. The expression of *abscisic acid-insensitive 3* (*OsABI3*), *OsABI4* and *OsABI5* was significantly up-regulated in germinating seeds of *OsHIPL1* mutants and NIL-*qsv3* line compared to IR26 plants. These results indicate that the regulation of seed vigour of *OsHIPL1* may be through modulating endogenous ABA levels and altering *OsABIs* expression during seed germination in rice. Meanwhile, we found that *OsHIPL1* interacted with the aquaporin *OsPIP1;1*, then affected water uptake to promote rice seed germination. Based on analysis of single-nucleotide polymorphism data of rice accessions, we identified a Hap1 haplotype of *OsHIPL1* that was positively correlated with seed germination. Our findings showed novel insights into the molecular mechanism of *OsHIPL1* on seed vigour.

Keywords: rice, seed vigour, *OsHIPL1*, ABA signalling, *OsPIP1;1*.

Introduction

Rice (*Oryza sativa* L.) is the staple food resource for half of the world's population. Rice direct seeding has been popularized because of its lower labour costs compared to the conventional transplanting of seedlings (Kumar and Ladha, 2011; Liu *et al.*, 2015). Seed germination and seedling establishment as key events in plant life activities are the important factors influencing the yield of direct seeding in rice (Gommers and Monte, 2018; Rajjou *et al.*, 2012). In the production fields of rice direct seeding, seed germination and seedling establishment could be delayed due to adverse environmental factors from paddy water surface or puddled soils, greatly increasing seedling mortality with a high risk of yield loss (Mahender *et al.*, 2015; Rao *et al.*, 2007). Seeds with high vigour have the power potential for rapid, uniform germination and the development of strong seedlings in rice fields, with the inhibition of weed growth (Foolad *et al.*, 2007; Wang *et al.*, 2010). Thus, the improvement of seed vigour is essential for the direct seeding of rice (Mahender *et al.*, 2015).

Seed vigour is a complex quantitative trait that is determined by the interactions between genetic and environmental factors. Many quantitative trait loci (QTL) for seed vigour, such as germination potential, germination index, germination percentage and seedling percentage, have been identified using the biparental mapping approach in rice (Fujino *et al.*, 2004, 2008; He *et al.*, 2019; Jiang *et al.*, 2011, 2017; Liu *et al.*, 2014; Xie *et al.*, 2014; Zeng *et al.*, 2021). Given these QTLs, some of the genes have been cloned and elucidated for seed vigour in rice. The

major *qLTG3-1* has been map-based cloned and its expression is tightly associated with vacuolation of the tissues covering the embryo during seed germination (Fujino *et al.*, 2008). *qSE3* encoding a K⁺ transporter *OsHAK21* was isolated to promote rice seed germination and seedling establishment under salinity stress (He *et al.*, 2019). Therefore, it is helpful to improve seed vigour of rice in breeding programme through further exploring and cloning the seed vigour-related genes, and elucidating their molecular mechanisms.

Viable seeds can rapidly germinate at favourable conditions, and its radicle protrudes the seed coats with growth of the seedlings (Bewley, 1997). Seed germination and seedling establishment are two important features that reflect the capacities of seed vigour to some extent. The process of seed germination is involved in a series of coordinated physiological and biochemical initiations, including the increase in oxygen and water uptake, the activation of the glycolysis, pentose phosphate pathway and tricarboxylic acid (TCA) cycle (He and Yang, 2013; Rajjou *et al.*, 2012). Previous studies show that well-germinated seeds are closely associated with the balance between internal reactive oxygen species (ROS) contents and the activities of ROS scavenging systems (Bailly *et al.*, 2008; El-Maarouf-Bouteau and Bailly, 2008; He *et al.*, 2019). High abundance of late embryogenesis abundant (LEA) protein and aquaporins has significant contributions to the hydraulic activity of cells and re-establishment of metabolism during seed germination (Footitt *et al.*, 2019; Vander Willigen *et al.*, 2006). The plant hormones, such as abscisic acid (ABA), gibberellin (GA) and auxin (IAA), also

take crucial roles in the regulation in cell homeostasis for seed germination and seedling establishment (Abe *et al.*, 2012; Debeaujon and Koornneef, 2000; Li *et al.*, 2016; Shu *et al.*, 2016).

It is well known that ABA as the major endogenous factor has been widely investigated involving the inhibition of seed germination (Penfield, 2017). The ABA levels in plants are maintained in strict homeostasis, including biosynthesis, degradation and conjugation, during various physiological processes (Palaniyandi *et al.*, 2015; Seiler *et al.*, 2011). The increase in ABA levels in seeds is controlled by ABA biosynthesis genes zeaxanthin epoxidase (*ZEP*) and 9-cis-epoxycarotenoid dioxygenases (*NCEDs*) (Eiji *et al.*, 2010). The decrease in ABA levels is regulated by ABA catabolism *CYP707A* family genes (Kushiro *et al.*, 2004). ABA content increases in seeds during the seed maturation and dormancy induction processes to activate the ABA signalling pathway (Shu *et al.*, 2016). ABA signalling is perceived by a set of receptors, which are members of the PYR1/PYL/RCAR family (Ma *et al.*, 2009; Park *et al.*, 2009). ABA binding to PYR1/PYL/RCAR complex leads to deactivation of protein phosphatase 2C, which releases and activates SnRK2 kinases (Chen *et al.*, 2020; Cutler *et al.*, 2010). Activated SnRK2s can phosphorylate ABA-responsive element (ABRE)-binding factors (ABFs) that promote the expression of ABA-dependent genes (Chen *et al.*, 2020; Sano and Marion-Poll, 2021; Song *et al.*, 2021). Among the identified ABF TFs (transcription factors), the B3 domain TF ABI3, the APETALA2 domain TF ABI4 and the basic leucine zipper (bZIP) TF ABI5 play central roles in regulating seed germination and early seedling growth (Ding *et al.*, 2014; Lopez-Molina *et al.*, 2001; Luo *et al.*, 2021). Loss-of-function *abi3* conferred reduced sensitivity to ABA during seed germination and early seedling growth (Ding *et al.*, 2014). ABI4 can directly combine with RbohD and vitamin C defective 2 (VTC2) and promotes ROS accumulation to decrease seed germination under salinity stress in *Arabidopsis* (Luo *et al.*, 2021). The germination of *abi5* mutants is insensitive to ABA, while *ABI5*-overexpressing plants are allergic to ABA (Finkelstein and Lynch, 2000; Lopez-Molina *et al.*, 2001). In rice, *OsiAGLU*, an indole-3-acetate beta-glucosyltransferase gene, was involved in the regulation of seed vigour through modulated *OsABIs* expressions in germinating seeds (He *et al.*, 2020).

Hedgehog-interacting protein (HIP) was identified as a hedgehog (Hh)-binding protein that is a target of Hh signalling (Chuang and McMahon, 1999). The Hh signalling pathway is essential for the development of diverse tissues during embryogenesis (Hammerschmidt *et al.*, 1997). Hh signalling is activated by binding of hedgehog protein to the multipass membrane protein Patched (Ptc) (Tabin and McMahon, 1997). Loss-of-function mutants in

HIP1 result in an up-regulation of Hh signalling in the mouse embryo, disrupting cell interactions essential for the normal morphogenesis of the lung and skeleton (Chuang *et al.*, 2003). Recently, the hedgehog-interacting protein-like 1 (HHIPL1) in human was reported as a secreted proatherogenic protein that enhances Hh signalling and regulates smooth muscle cell proliferation and migration (Aravani *et al.*, 2019). In *Arabidopsis*, it was reported that there were two hedgehog-interacting protein-like protein (HIPLs) belonging to glycosyl-phosphatidylinositol (GPI)-anchored proteins (GAPs) (Borner *et al.*, 2003). GAPs are involved in the generation of specialized cell surfaces and extracellular signalling molecules, likely targeting a specific subset of proteins to the cell surface for extracellular matrix remodelling and signalling (Borner *et al.*, 2002; Sherrier *et al.*, 1999). These imply that the HIPL might have potential roles in plants.

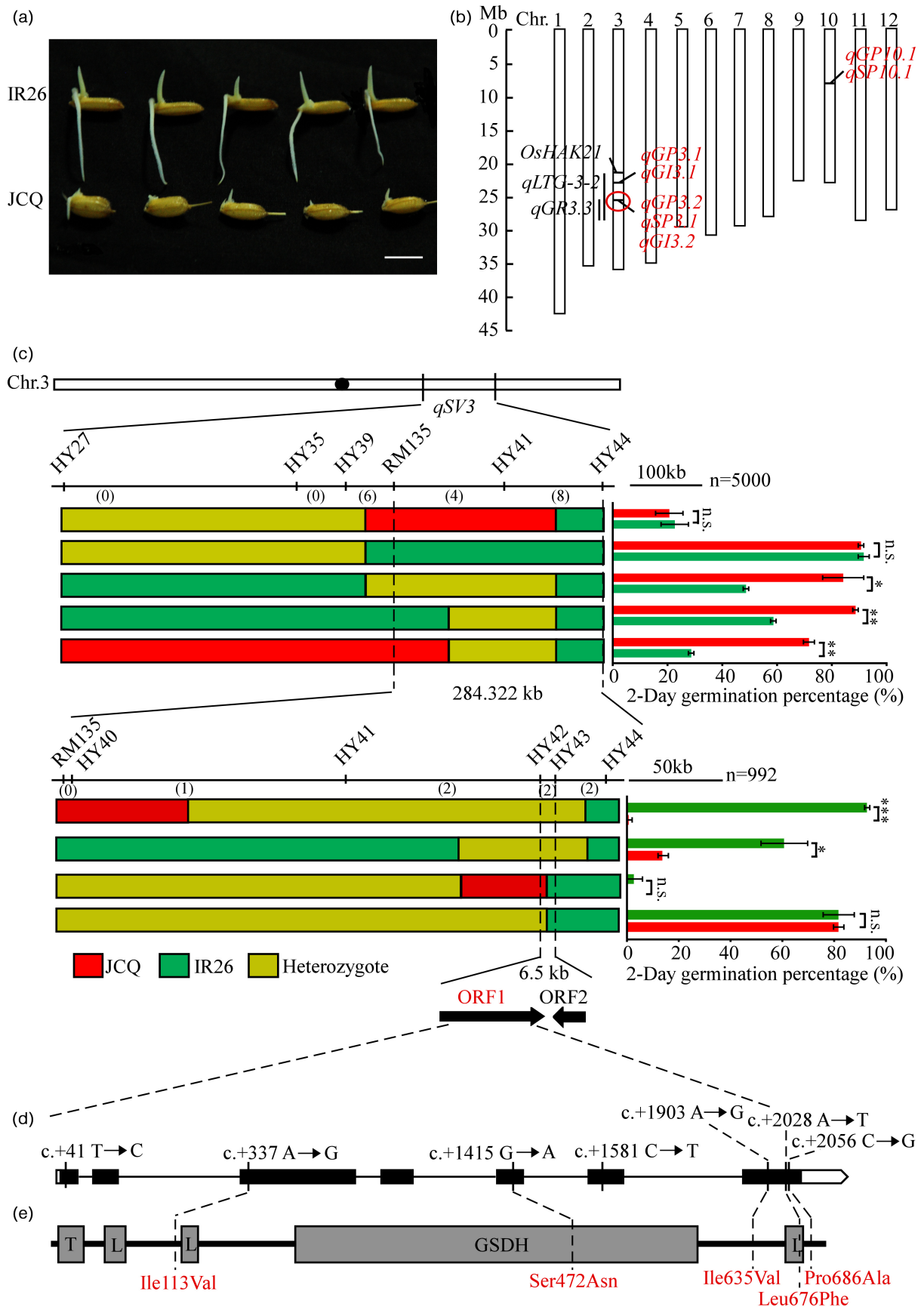
In our previous studies, a chromosome segment substitution lines (CSSL) population was structured based on the recipient parent IR26 and donor Jiucuiqing (JCQ) (Cheng *et al.*, 2016; He *et al.*, 2019). Here, we conducted QTL mapping of seed vigour using the CSSL population, and found a major locus *qSV3* on chromosome 3 improving seed germination and seedling establishment. The genetic and transgenic information showed that *OsHIPL1*, encoding a hedgehog-interacting protein-like 1 protein, was the causal gene of *qSV3*. Our results suggest that *OsHIPL1* acts in the regulation of seed vigour through the ABA pathway in seed germination. Moreover, we observed that *OsHIPL1* interacted with *OsPIP1;1* in rice. The application of *qSV3* may be useful in rice breeding programmes for improvement of rice seed vigour for direct seeding cultivation.

Results

Map-based cloning of *qSV3*

According to the previous report (He *et al.*, 2019), *indica* rice cultivar IR26 showed significantly high seed vigour under H₂O condition compared with *japonica* Jiucuiqing (Figures 1a and S1). To identify the elite genes controlling high seed vigour in IR26, a population consisting of 62 CSSLs was used for QTL identification and mapping. The seed germination percentage (GP), germination index (GI) and seedling percentage (SP) of 62 CSSLs, as well as their two parents, were assessed under H₂O condition respectively (Figure 1a, Tables S1 and S2). By single marker analysis (SMA), we identified seven QTLs, *qGP3.1*, *qGI3.1*, *qGP3.2*, *qGI3.2*, *qGP10.1*, *qSP3.1* and *qSP10.1*, for GP, SP and GI, respectively, and their positive alleles were derived from IR26 with an increase in seed vigour, except *qGP3.1* and *qGI3.1* (Figure 1b, Table S3). The *qGP3.2*, *qGI3.2* and *qSP3.1* were

Figure 1 Map-based cloning of *qSV3*. (a) Parental phenotype after 3 days after germination. Bar = 1 cm. (b) Physical mapping of QTLs related to seed vigour. Red QTLs identified based on CSSL population in this study and circle locus includes the major *qGP3.2*, *qGI3.2* and *qSP3.1*, which is named *qSV3*. The black QTLs have been reported previously and black lines show their physical regions. (c) The *qSV3* locus was fined within a 6.5 kb region between markers HY42 and HY43 on chromosome 3. Black circle represents the centromere. Numbers below the horizontal line are the number of recombinants. Red bars represent the JCQ genotype region; green and yellow bars represent IR26 genotype and heterozygous genotype respectively. Right: Germination percentage 2 days after germination. Each column presents the means \pm standard deviations of three biological replicates (* $P < 0.05$, ** $P < 0.01$ and *** $P < 0.001$) compared with the control by Student's *t*-test. n.s. represents no significance. Candidate genes ORF1 and ORF2 are LOC_Os03g48540 and LOC_Os03g48550 respectively. (d) Gene structure of ORF1. Empty boxes refer to 5' and 3' UTRs, black boxes to exons and the lines between boxes to introns. The SNPs from JCQ to IR26 in the *OsHIPL1* are shown by solid lines; SNP1, c.+41T→C; SNP2, c.+337A→G; SNP3, c.+1415G→A; SNP4, c.+1581C→T; SNP5, c.+1903A→G; SNP6, c.+2028A→T; and SNP7, c.+2056C→G. (e) Protein structure of ORF1. T, L and GSDH represents the transmembrane domain, the low complexity region and glucose/sorbose dehydrogenase domain predicted respectively. Dashed lines show the positions of two amino acid transitions.



mapped to be tightly associated with marker RM3513 on chromosome 3, integrated as a *qSV3* locus (Table S3). The *qGP10.1* and *qSP10.1* were mapped to be tightly associated with the marker RM5348 on chromosome 10, integrated as a *qSV10* locus (Table S3). Since the *qSV3* showed higher contribution to seed vigour with 37.75% of average phenotypic variation (APV) of GP, 21.74% of APV of SP and 88.52% of APV of GI, it was further analysed in this study.

The residual heterozygous line CSSL10, containing the allele (*qsv3*) from parent Jiucaiqing (Figure S2A, Table S1) with the low GP, SP and GI, was selected for confirming *qSV3* locus. A segregation population consisting of 120 individuals was developed by self-fertilization of CSSL10, and their GP at 2 days after imbibition showed bimodal characteristic distribution (Figure S2B), suggesting the presence of a major gene. Inclusive composite interval mapping (ICIM) showed that there was a significant QTL of GP between markers HY27 and HY44, with 55.48% of phenotypic variation (Figure S2C). A total of 5000 individuals from the BC₆F₄ population were used to narrow down the *qSV3* locus into a genomic region between the markers RM135 and HY44 (Figure 1c). A total of 992 individuals of the BC₆F₅ population were used to further delimit the *qSV3* locus in an approximately 6.5 kb region between the markers HY42 and HY43 (Figure 1c).

In this region, two genes, *LOC_Os03g48540* (*ORF1*) and *LOC_Os03g48550* (*ORF2*), were predicted in the Rice Annotation Project Database (<http://rice.uga.edu/index.shtml>). *ORF1* encodes a hedgehog-interacting protein-like 1 protein, designated as *Oshipl1*, with seven exons and six introns, and *ORF2* encodes one retrotransposon protein. To define the candidate gene of *qSV3*, the cDNA of these two *ORFs* was cloned from IR26 and Jiucaiqing, respectively, and sequenced for comparison. There were no nucleotide differences in *ORF2* between IR26 and Jiucaiqing (Figure S3), but seven single-nucleotide polymorphisms (SNPs) (SNP1–SNP7) were found in *ORF1* (*Oshipl1*) (Figure 1d). Among these SNPs, five SNPs caused amino acid residue changes between IR26 and Jiucaiqing. SNP2 in the third exon of *Oshipl1* caused amino acid residue change from isoleucine in IR26 to valine in Jiucaiqing (Ile1137Val); SNP3 in the fifth exon of *Oshipl1* caused serine to asparagine (Ser472Asn); and SNP5, SNP6 and SNP7 in the seventh exon of *Oshipl1* caused isoleucine to valine (Ile635Val), leucine to phenylalanine (Lue676Phe) and proline to alanine (Pro686Ala) respectively (Figure 1d–e).

SMART (<http://smart.embl-heidelberg.de/>) results showed that *Oshipl1* contains 699 amino acids with one transmembrane domain, three low complexity regions and one glucose/sorbosone dehydrogenase (GSDH) domain. SNP3 and SNP6 were predicted to locate in GSDH domain and the third low complexity region respectively (Figure 1e). Thus, *Oshipl1* was considered as a causal gene for *qSV3*.

Confirmation of *Oshipl1* as *qSV3*

Three homozygous knockout mutants (*Oshipl1a*, *Oshipl1b* and *Oshipl1c*, T₂) were developed in the background of IR26 through the CRISPR/Cas9 system (Figure 2a). The *Oshipl1a* contained a 'T' and an 'A' insertion in the first and second exons of *Oshipl1*, respectively; the *Oshipl1b*, an 'A' insertion in the first and second exons of *Oshipl1*, respectively; and the *Oshipl1c*, a '27bp' deletion and a 'C' insertion in the first and second exons of *Oshipl1* respectively (Figure 2a). Based on these nucleotide sequences, the amino acid sequence of *Oshipl1* was predicted to contain only 64, 9 and 85 amino acids in *Oshipl1a*, *Oshipl1b*

and *Oshipl1c* mutants, respectively, which were caused by premature termination (Figure 2b). This result indicates that the mutants lacked *Oshipl1* gene. Germination assays showed that the GP, SP and GI of *Oshipl1a*, *Oshipl1b* and *Oshipl1c* mutants were significantly reduced compared with those of IR26 (Figure 2c–f), suggesting that the disruptions of *Oshipl1* gene significantly decreased seed vigour.

A near isogenic line (NIL), containing a small chromosomal segment around *qsv3* from Jiucaiqing (NIL-*qsv3*), was developed in IR26 genetic background. The NIL-*qsv3* showed a lower seed vigour than IR26 (Figure S4). To further confirm whether *Oshipl1* is the causal gene of *qSV3*, we performed a genetic complementation test in the NIL-*qsv3* background. The *Oshipl1* expression levels in three complementation lines (COM-1, COM-2 and COM-3, T₂) were 7-fold, 9-fold and 10-fold higher than those in NIL-*qsv3* respectively (Figure S5A). Germination assays showed that the GP, SP and GI of complementation lines were significantly increased, compared with NIL-*qsv3* (Figure 2g–j), indicating that the allele (*Oshipl1*) of IR26 compensates the defective function of *qsv3* allele on seed vigour.

We further generated *Oshipl1* overexpression lines (OE-1, OE-2 and OE-3, T₂) containing the 35S promoter fused to the *Oshipl1*-coding region from IR26 transformed into *japonica* Zhonghua 11 (ZH11). The *Oshipl1* expression levels in OE-1, OE-2 and OE-3 lines were 9-fold, 13-fold and 17-fold higher than that in ZH11, respectively (Figure S5B). Seed germination assays showed that the GP, SP and GI of the overexpression lines were significantly increased compared with those of ZH11 (Figure 2k–n). It indicates that *Oshipl1* is a positive regulator for seed vigour in rice.

Expression patterns of *Oshipl1* and subcellular localization

By the quantitative RT-PCR (RT-qPCR) approach, the expression patterns of the *Oshipl1* gene were analysed in various tissues, and germinating and developing seeds in IR26. There was a relatively higher expression of *Oshipl1* identified in the root, compared with that in the stem, leaf, sheath, internode and spike (Figure 3a). During seed germination, the transcript levels of *Oshipl1* were gradually increased at the early stage (0–30 h after imbibition), then decreased at the late stage (36–72 h after imbibition) (Figure 3b). During seed development, the expression levels of *Oshipl1* gradually increased from 0 to 35 days after flowering (Figure 3c). The specific expression of *Oshipl1* suggested that it might play a role in modulating seed vigour in rice.

To determine the subcellular localization of *Oshipl1*, a recombinant *Oshipl1* protein-tagged green fluorescent protein (GFP) at the C terminus under the control of the 35S promoter was constructed and expressed transiently in rice protoplasts and *N. benthamiana* leaves. The GFP-tagged *Oshipl1* was found to be mainly localized in the plasma membrane and nucleus in rice protoplasts and *N. benthamiana* leaf epidermal cells (Figure 3d–e).

Oshipl1 is involved in ABA-mediated processes possibly during seed germination

To explore the regulatory mechanism of *Oshipl1* on seed vigour, the RNA-seq analysis was performed between IR26 and NIL-*qsv3* at the 12th hour (h) after imbibition. A total of 3186 differently expressed genes (DEGs) were identified, including 1432 up-regulation and 1754 down-regulation, in NIL-*qsv3* compared to IR26 (*P*-value < 0.05, fold change ≥ 2) (Table S4). Twelve DEGs,

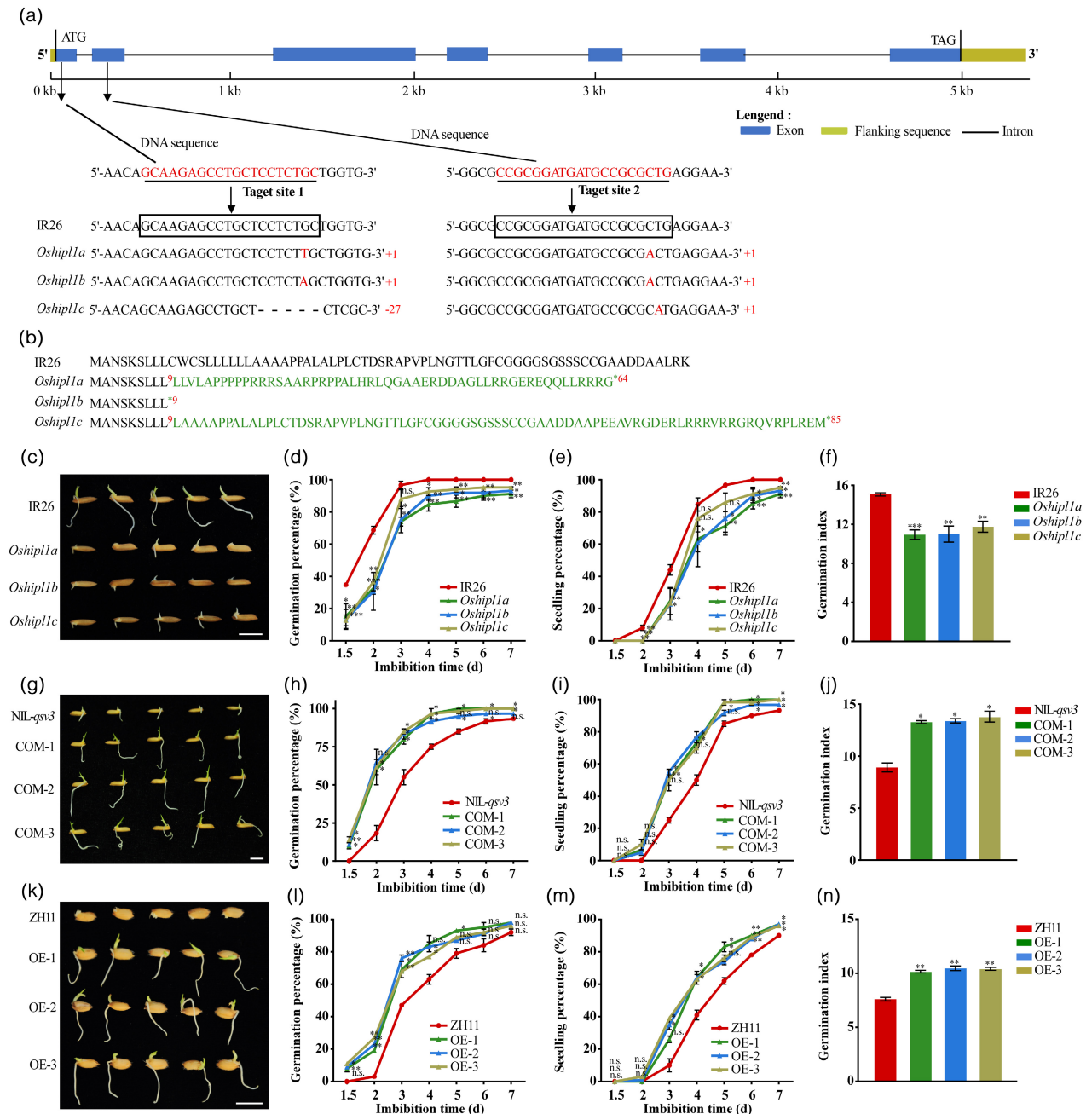


Figure 2 Functional analysis of *OsHIPL1* during seed germination. (a) Target sites are marked in red. Sequences in boxes are the target sequences in the wild type (WT). Black dashes represent the deleted bases and inserted nucleotides are indicated with red uppercase letters. (b) Analysis of the *OsHIPL1* protein sequence in the wild-type (WT) and *OsHIPL1*-knockout lines. (c) Photographs of germinated seeds of *Oshipl1* mutants and IR26 (control) after 3 days after germination. (d–f) Comparison of germination percentage (d), seedling percentage (e) and germination index (f) between *Oshipl1* mutants and IR26. (g) Photographs of germinated seeds of COM lines and *NIL-qsv3* (control) after 3 days after germination. (h–j) Comparison of germination percentage (h), seedling percentage (i) and germination index (j) between COM lines and *NIL-qsv3*. (k) Photographs of germinated seeds of OE lines and ZH11 (control) after 3 days after germination. (l–n) Comparison of germination percentage (l), seedling percentage (m) and germination index (n) between OE lines and ZH11. Bar = 1 cm. Each column presents the means \pm standard deviations of three biological replicates. * $P < 0.05$, ** $P < 0.01$ and *** $P < 0.001$ compared with the control by Student's *t*-test.

including five ABA-related genes, six IAA-related genes and one ascorbate peroxidase gene, were randomly selected for their expression by the RT-qPCR approach in germinating seed of IR26 and *NIL-qsv3*. It was observed that there was a consistent expression pattern for those DEGs by the RNA-Seq and RT-qPCR

approach in germinating seeds between IR26 and *NIL-qsv3* seeds (Figure S6).

All DEGs were analysed based on the gene ontology (GO) and the Kyoto Encyclopedia of Genes and Genomes (KEGG). GO results showed that the pathways involved in abiotic stimulus in

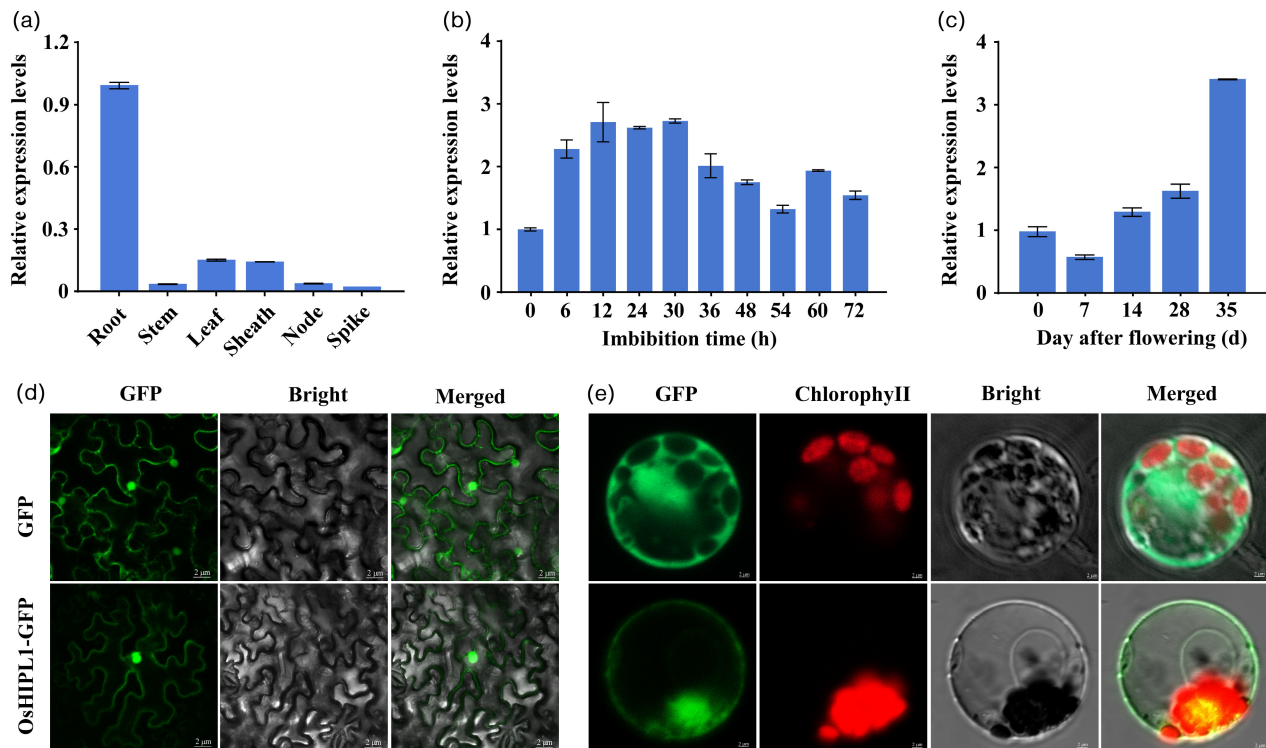


Figure 3 Expression patterns of *OsHIPL1* and subcellular localization in rice. Expression pattern of *OsHIPL1* in various tissues (a), germinating stages (b) and seed developmental stages (c) in IR26 using the RT-qPCR approach. The expression of *OsHIPL1* was normalized to that of *OsActin* gene control. The relative expression levels were represented by fold change relative to the expression level of *OsHIPL1* at 0 days after flowering or 0 h imbibition stage under H₂O treatment. Each column represents the means \pm standard deviation. (d) Subcellular localization of *OsHIPL1* in *N. benthamiana* leaves. (e) Subcellular localization of *OsHIPL1* tagged at the C terminus with GFP in rice protoplasts.

biological process (BP), DNA binding in molecular function (MF) and cell periphery in cellular component (CC) were significantly enriched (Figure S7). KEGG results showed that many DEGs between IR26 and NIL-*qsv3* were involved in the plant hormone signal transduction including ABA, IAA, GA, brassinosteroid (BR), ethylene (ET), cytokinin (CK) and jasmonic acid (JA) (Figure S8A, Table S5).

ABA plays a crucial role in the control of seed dormancy and germination (Finkelstein *et al.*, 2008; Rajjou *et al.*, 2012). Our RNA-Seq showed that 18 DEGs were related to ABA metabolism, including ABA signal transduction genes (12), ABA response genes (4), ABA biosynthesis gene (1) and ABA inducible gene (1) (Figure S8B). To examine whether the function of *OsHIPL1* is dependent on the ABA, we investigated the expression levels of *OsHIPL1* under ABA treatments during seed germination. The RT-qPCR analysis indicated that *OsHIPL1* expression was significantly induced by ABA during seed imbibition (Figure S9). These results suggest that the regulation of *OsHIPL1* on seed vigour may be involved in ABA-mediated processes during seed germination in rice.

OsHIPL1 regulates ABA metabolism and signalling during seed germination

To investigate whether *OsHIPL1* is involved in ABA responses, we investigated the IR26 and two mutants *Oshipl1a* and *Oshipl1b* in response to exogenous ABA (0, 1 and 3 μ M) during seed germination. In the presence of ABA, the seed vigour of *Oshipl1* mutants and IR26 was significantly reduced (Figure 4a–d), and the seed vigour of *Oshipl1* mutants declined more than that of

IR26 plants. Furthermore, we investigated the COM-1, COM-2 and NIL-*qsv3* lines in response to exogenous ABA (0, 1 and 3 μ M) during seed germination. In the presence of ABA, the seed vigour of complementation and NIL-*qsv3* lines were significantly reduced. Moreover, the seed vigour of the complementation lines declined less than that of NIL-*qsv3* line (Figure 4e–h). This suggests that the function of *OsHIPL1* can relieve the inhibited effect of exogenous ABA during seed germination.

The *Oshipl1* mutants and NIL-*qsv3* line exhibit delayed seed germination, suggesting that the mutants and NIL-*qsv3* line may accumulate more ABA content. We measured the ABA contents among IR26, NIL-*qsv3*, *Oshipl1a* and *Oshipl1b* lines using an ultra-performance liquid chromatography–tandem mass spectrometry (LC-MS/MS) approach during seed germination. The results demonstrated that the ABA levels were significantly increased in germinating seeds of *Oshipl1* mutants and NIL-*qsv3* line compared to those in IR26 (Figure 5a), indicating that *OsHIPL1* was involved in ABA internal metabolism. Meanwhile, we evaluated the expression levels of pivotal ABA metabolism genes (Figure 5b, c), including *OsZEP* and *OsNCEDs* (ABA biosynthesis) and *OsABA8oxs* (ABA degradation) among IR26, *Oshipl1* mutants and NIL-*qsv3* line at 12 h after imbibition. The expression levels of *OsZEP* and *OsNCED4* were significantly up-regulated in *Oshipl1* mutants and NIL-*qsv3* line, compared with IR26, and the expression levels of *OsNCED1*, *OsNCED3* and *OsNCED5* were up-regulated in *Oshipl1* mutants while not in NIL-*qsv3* line (Figure 5b). The expression levels of ABA degradation gene *OsABA8ox3* were markedly down-regulated in *Oshipl1* mutants and NIL-*qsv3* line, compared with IR26, and the expression levels

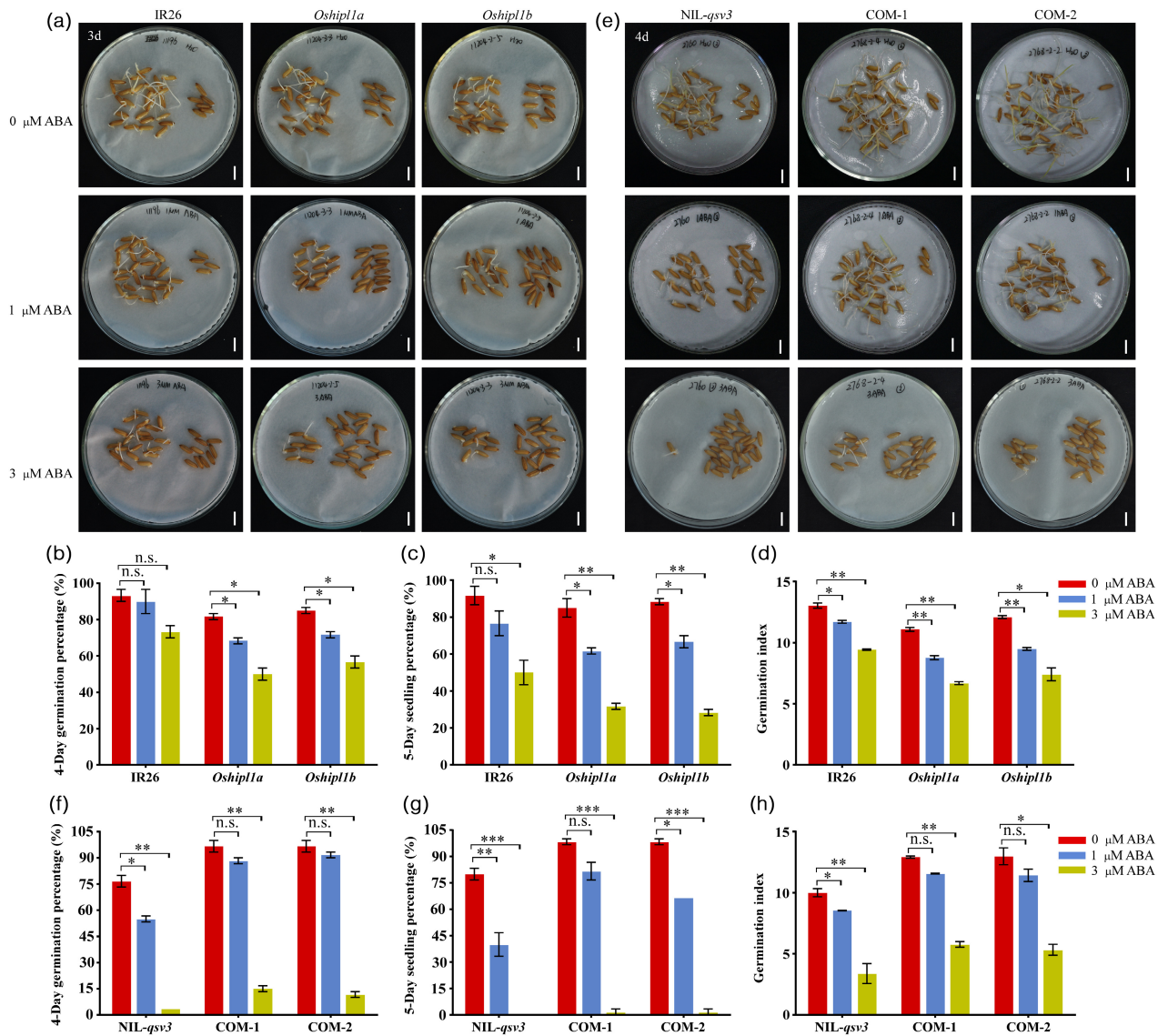


Figure 4 Effects of ABA treatments on *Oshipl1* during seed germination. (a) Photographs of germinated seeds of *Oshipl1* mutants and IR26 after 3 days after germination with 0, 1 and 3 μM ABA treatments. (b–d) Comparison of germination percentage (b), seedling percentage (c) and germination index (d) of *Oshipl1* mutants and IR26 in the presence of ABA. (e) Photographs of germinated seeds of COM lines and NIL-*qsv3* after 4 days after germination with 0, 1 and 3 μM ABA treatments. (f–h) Comparison of germination percentage (f), seedling percentage (g) and germination index (h) of COM lines and NIL-*qsv3* in the presence of ABA. Bar = 1 cm. Each column presents the means ± standard deviations of three biological replicates. * $P < 0.05$, ** $P < 0.01$ and *** $P < 0.001$ compared with the control by Student's *t*-test. n.s. represents no significance.

of *OsABA8ox1* were down-regulated in NIL-*qsv3* line while not in *Oshipl1* mutants (Figure 5c). Differential expression levels of *OsZEP*, *OsNCED4* and *OsABA8ox3* among IR26, *Oshipl1* mutants and NIL-*qsv3* line could well explain the increased ABA content of *Oshipl1* mutants and NIL-*qsv3* seeds.

Our global analysis of transcripts in imbibed seeds indicated that the ABA signalling-related genes, such as *OsABI4*, *OsBZIP23* and *OsBZIP12*, were significantly induced in NIL-*qsv3* line compared to those of IR26 plants (Figure S8B). We speculate that the regulation of *Oshipl1* on seed vigour might involve in ABA signalling during seed germination in rice. Therefore, we checked the transcript abundance of several identified ABA signalling-related genes during seed germination, including *OsABI3*, *OsABI4* and *OsABI5* (Finkelstein and Lynch, 2000; Kang et al., 2002;

Lopez-Molina et al., 2001; Söderman et al., 2000). The transcript levels of *OsABI3*, *OsABI4* and *OsABI5* were significantly increased in NIL-*qsv3* line and *Oshipl1* mutants during seed germination compared with those of IR26 (Figure 5d–f). The expression levels of *OsABI3*, *OsABI4* and *OsABI5* were further evaluated in the NIL-*qsv3* line and IR26 plants during seed germination under ABA treatment. We observed that the expression levels of *OsABI3*, *OsABI4* and *OsABI5* were approximately 2–3 fold higher in NIL-*qsv3* seeds than that without ABA, but weakly induced in IR26 seeds following ABA treatment (Figure 5g–i). These data demonstrate that the disruption of *Oshipl1* alters the expression of *OsABI3*, *OsABI4* and *OsABI5*, and their continuously higher expressions in germinating seeds caused low seed vigour in *Oshipl1* mutants and NIL-*qsv3* line in rice.

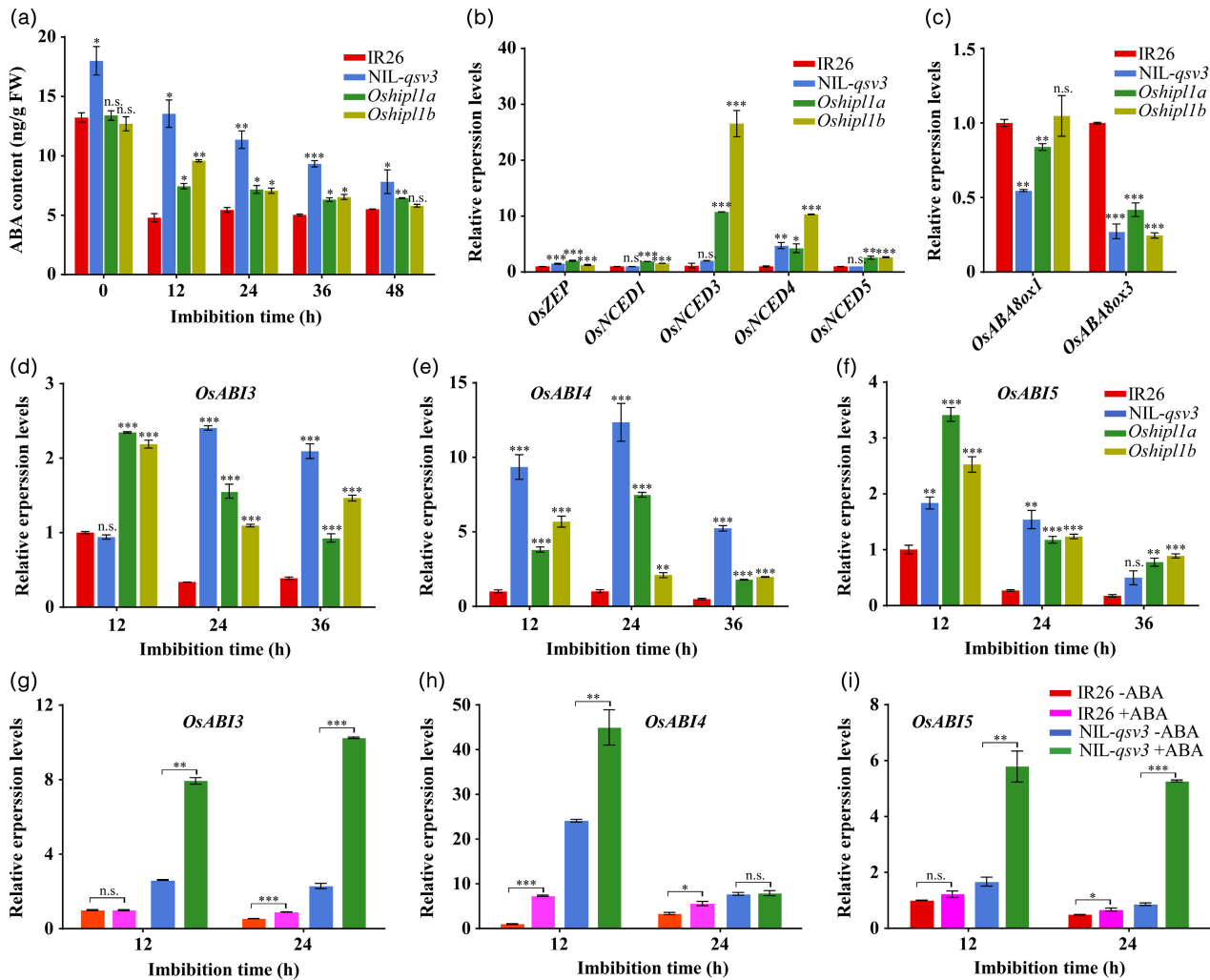


Figure 5 *OshIPL1* altering the contents of ABA and expressions of ABA signalling genes *OsABIs* during seed germination. (a) The contents of ABA in germinated seeds of IR26, NIL-*qsv3* and *Oshipl1* mutants. (b, c) Transcription levels of ABA biosynthesis genes (*OsZEP*, *OsNCED1*, *OsNCED3*, *OsNCED4* and *OsNCED5*) (b) and ABA degradation genes (*OsABA8ox1* and *OsABA8ox3*) (c) among IR26, *Oshipl1* mutants and NIL-*qsv3* line at the 12 h seeds after imbibition. The relative expression levels were represented by fold change relative to the expression levels of IR26 at 12h after imbibition. (d–f) Comparison of *OsABI3* (d), *OsABI4* (e) and *OsABI5* (f) expression in germinated seeds among NIL-*qsv3*, *Oshipl1* mutants and IR26 (control) during seed germination. The relative expression levels were represented by fold change relative to the expression levels of IR26 at 12 h after imbibition. (g–i) Expressions of *OsABI3* (g), *OsABI4* (h) and *OsABI5* (i) in germinated seeds were induced at ABA treatments in IR26 and NIL-*qsv3* using the RT-qPCR approach. The relative expression levels were represented by fold change relative to the expression levels of IR26 without ABA. The expression of *OshIPL1* was normalized to that of *OsActin* gene control.

OsHIPL1 interacts with aquaporin OsPIP1;1 to improve seed germination

To further understand the molecular mechanism of regulation by *OshIPL1* on seed vigour in rice, we identified the interacting proteins through a yeast two-hybrid assay with *OshIPL1* as bait. Of the identified 22 candidates (Table S6), 5 candidate proteins were subsequently confirmed by retransformation into yeast, including aquaporin OsPIP1;1 (Figure 6a).

To further confirm the *OshIPL1*-OsPIP1;1 interaction, the bimolecular fluorescence complementation (BiFC) and luciferase (LUC) assays were conducted. The yellow fluorescent protein (YFP) signals were only observed on the plasma membrane of *N. benthamiana* leaves when cYFP-*OshIPL1* was co-infiltrated with nYFP-OsPIP1;1 (Figure 6b). Meanwhile, only co-expression of

cLUC-*OshIPL1* and nLUC-*OsPIP1;1* in tobacco leaves could reconstitute LUC activity compared with the various negative controls (Figure 6c). These results demonstrate that *OshIPL1* could interact with *OsPIP1;1*.

To investigate whether *OshIPL1* affects water uptake during seed germination, we tested the water content of the germinating seeds. The water content of *Oshipl1* mutants was significantly reduced compared with that of IR26 (Figure 6d). By contrast, the water content of COM and OE lines was significantly increased compared with that of NIL-*qsv3* line and ZH11, respectively (Figure 6e,f). These data indicate that *OshIPL1* promotes uptake of water during seed germination.

The *OsPIP1;1* expression was also tested. A reduction in the transcript levels of *OsPIP1;1* in *Oshipl1* mutants was observed compared with that in IR26, and an increase in the relative

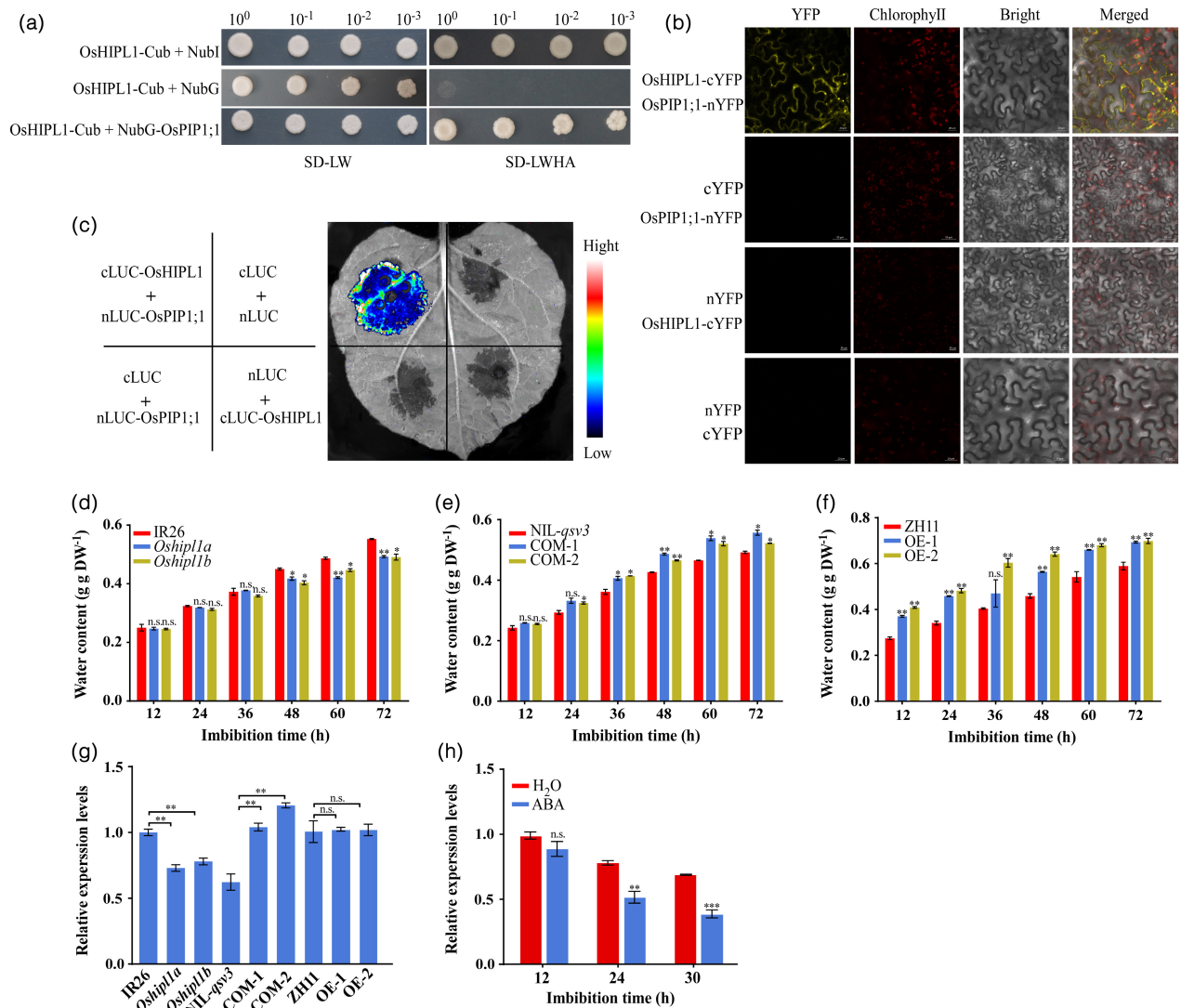


Figure 6 *OsHIPL1* interacts with *OsPIP1;1* and promotes water uptake during seed germination. (a) Yeast two-hybrid screening assay. Interaction of *OsHIPL1* with *OsPIP1;1* is indicated by the ability of yeast cells to grow on dropout medium lacking Leu, Trp, His and Ade for 4 days after plating. CUB, C-terminal half of ubiquitin; Nub, N-terminal half of ubiquitin; NubG, negative control with a point mutation in Nub; NubI, positive control. The experiments were repeated three times with similar results. (b) Bimolecular fluorescence complementation (BiFC) assay. The fluorescence resulted from the complementation of the C-terminal portion of YFP fused to *OsHIPL1* (*OsHIPL1*-cYFP) with the N-terminal portion of YFP fused to *OsPIP1;1* (*OsPIP1;1*-nYFP). Fluorescence was observed in tobacco leaf epidermal cells. (c) Firefly luciferase (LUC) complementation imaging assay. cLUC-*OsHIPL1* and nLUC-*OsPIP1;1* with the control vector were co-infiltrated into *N. benthamiana* leaves. LUC images were captured at 48 h after infiltration. (d–f) Water contents of *Oshipl1* mutants and IR26 (d), COM lines and NIL-*qsv3* (e) and OE lines and ZH11 (f) during seed germination. (g) Comparison of the transcription levels of *OsPIP1;1* among IR26, *Oshipl1* mutants, NIL-*qsv3*, COM lines, ZH11 and OE lines at 24 h after imbibition using the RT-qPCR approach. The relative expression levels were represented by fold change relative to the expression levels of IR26 or ZH11. The expression of *OsPIP1;1* was normalized to that of *OsActin* gene control. (h) Transcription levels of *OsPIP1;1* response to ABA treatments in germinated seeds were conducted using the RT-qPCR approach. The relative expression levels were represented by fold change relative to the expression level of *OsPIP1;1* at 12 h after imbibition without ABA. Each column presents the means \pm standard deviations of three biological replicates. * $P < 0.05$, ** $P < 0.01$ and *** $P < 0.001$ compared with the control by Student's *t*-test. n.s. represents no significance.

expression levels of *OsPIP1;1* in COM lines was observed compared with that in NIL-*qsv3* line (Figure 6g). There were no obvious differences in the expression levels of *OsPIP1;1* of OE lines compared with that in wild-type ZH11.

It was well-known that ABA could regulate the expression of aquaporin genes in a variety of plants (Jang *et al.*, 2004; Mariaux *et al.*, 1998; Suga *et al.*, 2002; Zhu *et al.*, 2005). Therefore, the transcript levels of *OsPIP1;1* were tested during seed germination

at the treatments with ABA. The results showed that the expression of *OsPIP1;1* was significantly reduced during seed germination in the presence of ABA (Figure 6h), suggesting ABA may inhibits *OsPIP1;1* expression.

Genetic variation in the regulatory region of *OsHIPL1*

To identify the allelic constitution of *OsHIPL1*, 192 rice accessions of the Rice Diversity Panel 1 (RDP1) were selected to be evaluated

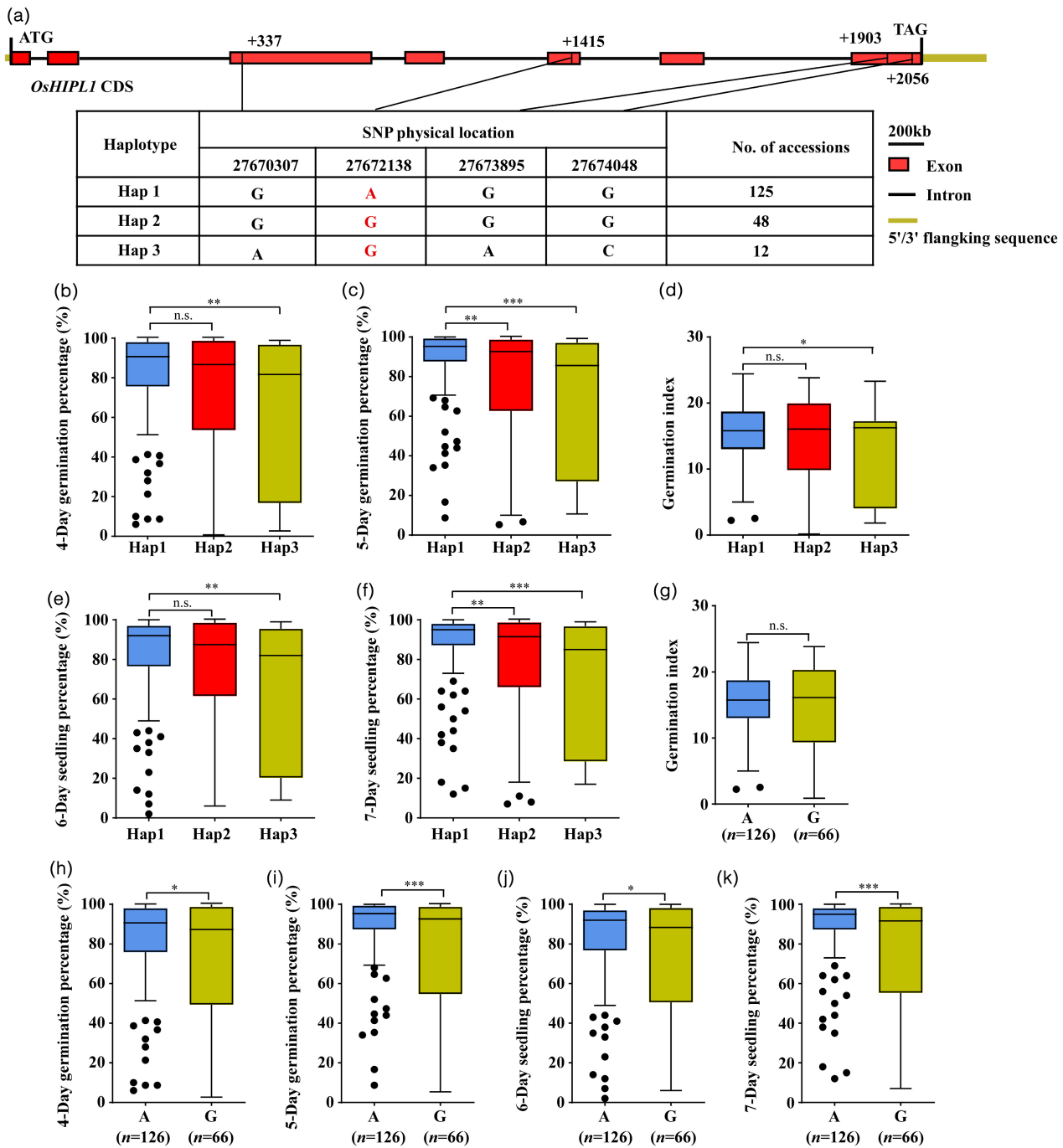


Figure 7 Haplotypes of *OsHIPL1* associated with seed vigour in rice. (a) Haplotypes of *OsHIPL1* were identified in the full-length CDS of the gene. Red boxes represent the exon; solid lines represent the intron; yellow boxes represent 5'UTR and 3'UTR. (b–f) Comparison of the germination percentage, seedling percentage and germination index between accessions harbouring different haplotypes. (g–k) Comparison of the germination percentage, seedling percentage and germination index of accessions harbouring 1415A or 1415G SNP. The number of rice accessions is listed in brackets. (* $P < 0.05$; ** $P < 0.01$, *** $P < 0.001$ compared with the control by Student's *t*-test. n.s. represents no significance).

by GP, SP and GI during seed germination (Table S7). Four SNPs were identified in the coding region of *OsHIPL1* and three haplotypes (Hap1, Hap2 and Hap3) were detected (Figure 7a). The 4- and 5-day GP, 6- and 7-day SP of Hap1 were significantly higher than those of Hap2 and Hap3 (Figure 7b–f), suggesting Hap1 is superior allele for seed vigour. These four SNPs, SNP-3.27670307., SNP-3.27672138., SNP-3.27673895. and SNP-

3.27674048., were consistent with SNP2, SNP3, SNP5 and SNP7 identified between IR26 and Jiucaiqing (Table S7) respectively. Of them, the amino acid residue change in SNP3 is from serine to asparagine (Ser1415Asn) in GSDH domain (Figure 1d,e), suggesting that SNP3 may be significantly associated with seed vigour. To confirm this hypothesis, we further analysed the seed vigour of 192 rice accessions. The results showed that 126 rice

accessions harbouring 'A' SNP exhibited higher GP and SP than did 66 rice accessions with 'G' SNP (Figure 7g–k). These results indicated that Hap1 and SNP3 of *qSV3* have significantly positive correlation with seed vigour in rice.

OshIPL1 increases the seed vigour of direct seeding rice under greenhouse and field

To investigate the application of *OshIPL1* for direct seeding, seedling establishment and seedling growth were compared among IR26, *Oshipl1* mutants, NIL-*qsv3*, the COM lines and ZH11 and OE lines when seeds were directly sown in soil. In the greenhouse, the SP, root length, shoot length and basal shoot diameter were significantly higher in IR26 than in NIL-*qsv3* line and *Oshipl1* mutants (Figure 8). Moreover, the COM lines

exhibited a significant increase in the SP, shoot length, shoot length and basal shoot diameter compared with those of NIL-*qsv3* line, and the OE lines significantly increase in the shoot length and basal shoot diameter compared with those of ZH11 (Figure 8). Meanwhile, there were the decreases in the SP of NIL-*qsv3* line and *Oshipl1* mutants compared with those of IR26 and the increases in the SP of COM lines compared with those of NIL-*qsv3* line under the field (Figure S10). Agronomic traits were similar between IR26, *Oshipl1* mutants, NIL-*qsv3* and COM lines, including plant height, effective tillers, 1000-grain weight, panicle length, setting percentage and grain per panicle (Figure S11). These results suggested that *qSV3* could improve the performance of plants directly seeded without adverse influence on other agronomic traits.

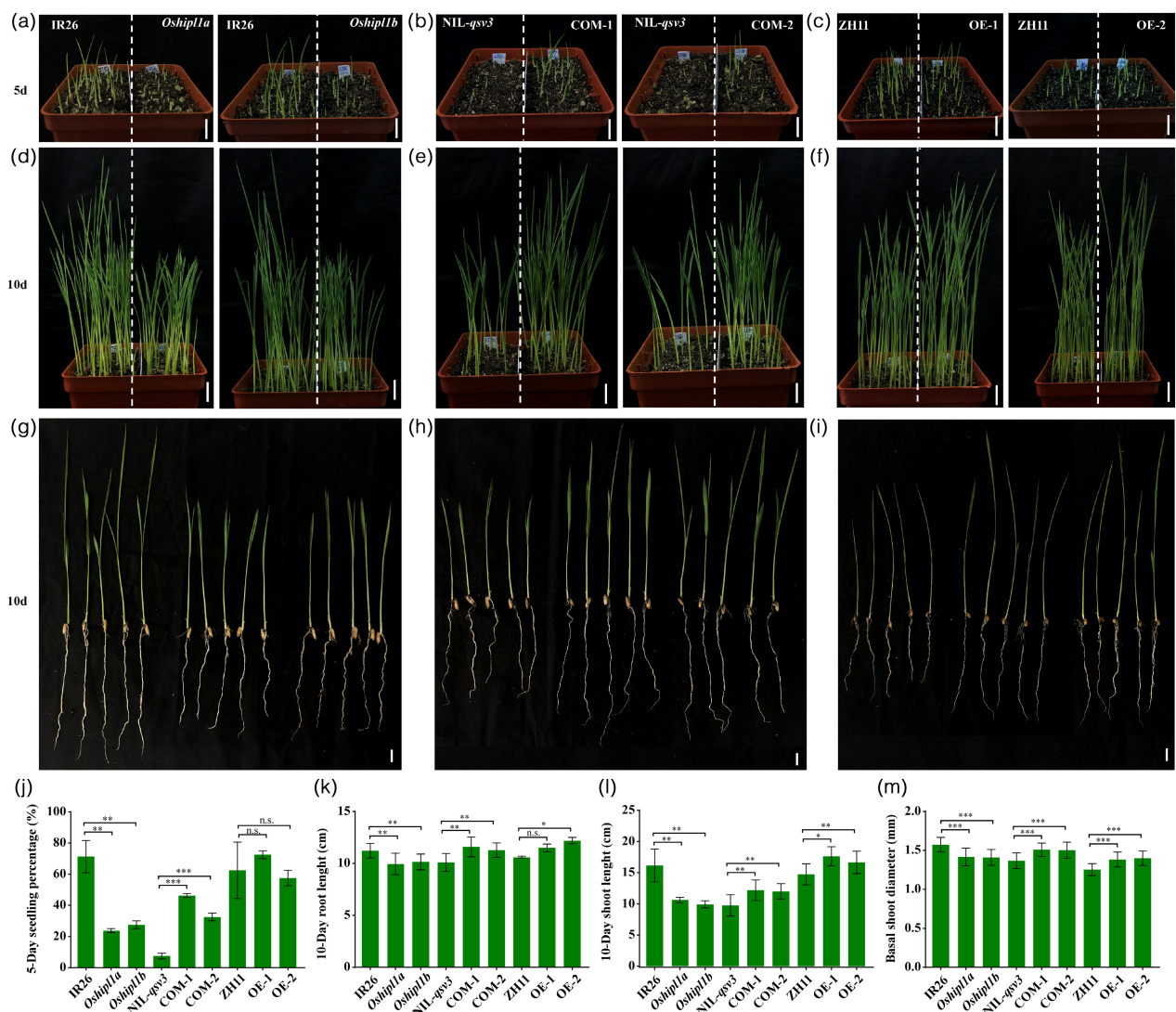


Figure 8 Effects of *OshIPL1* on seedling growth under direct seeding in soil. (a–c) Photographs of seedling establishment of *Oshipl1* mutants and IR26 (a), COM lines and NIL-*qsv3* (b), and OE lines and ZH11 (c) at 5 days after sowing. (d–f) Photographs of seedling growth of *Oshipl1* mutants and IR26 (d), COM lines and NIL-*qsv3* (e) and OE lines and ZH11 (f) at 10 days after sowing. (g–i) Photographs of representative seedlings of *Oshipl1* mutants and IR26 (g), COM lines and NIL-*qsv3* (h) and OE lines and ZH11 (i) at 10 days after sowing. (j–m) Comparison of seedling percentage (j), root length (k), shoot length (l) and base diameter (m) among IR26, *Oshipl1* mutants, NIL-*qsv3*, COM lines, ZH11 and OE lines. Bars = 1 cm. Each column presents the means \pm standard deviations of three biological replicates. * $P < 0.05$, ** $P < 0.01$ and *** $P < 0.001$ compared with the control by Student's *t*-test. n.s. represents no significance.

Discussion

Seed vigour is an important trait for production of direct seeding of rice, which could be evaluated by the speed and uniformity of seed germination, and seedling establishment (Bewley *et al.*, 2013; Rajjou *et al.*, 2012). In this study, seven QTLs were identified, related to GP, SP and GI of rice seed vigour, using one CSSL population under H₂O condition respectively. Three major QTLs *qGP3.2*, *qGI3.2* and *qSP3.1* were integrated into a *qSV3* locus, and further confirmed by the segregation population derived from the residual heterozygous CSSL10 line. Compared with the reported QTLs, the *qSV10* (*qGP10.1* and *qSP10.1*) is a novel QTL for seed vigour; the *qSV3* is located in the downstream of *OsHAK21* (He *et al.*, 2019), co-localized with *qGR3.3* identified under H₂O condition (Zeng *et al.*, 2021) and *qLTG-3-2* under low-temperature stress (Fujino *et al.*, 2004). As the seed vigour of *Oshipl1* mutants and NIL-*qsv3* was significantly reduced under abiotic stresses, and the seed vigour of COM lines was restored (Figures S12 and S13), it implied that *qSV3* could also respond to abiotic stresses, with similar function of *qLTG-3-2* reported (Fujino *et al.*, 2004). Its molecular regulation mechanism and application in improvement of seed vigour in rice breeding deserve to be further investigated.

We isolated and characterized the causal gene *OsHIPL1* of *qSV3* in this study, which encodes a hedgehog-interacting protein-like 1 protein. Human HHPL1 was shown to positively regulate hedgehog signalling (Aravani *et al.*, 2019) and the hedgehog signalling in mammalian was reported to modulate the embryogenesis, cancer and lifespan (Kato and Kato, 2006; Arraf *et al.*, 2020; Rallis *et al.*, 2020; Jiang, 2021). A phylogenetic tree analysis shows that HIPL1 protein is highly conserved in plants, such as rice, *Brachyodium stacei*, maize, sorghum and *Arabidopsis* (Figure S14). Moreover, the function of HIPL1 protein is still unknown in plants. Protein structure analysis showed that *OsHIPL1* contained one transmembrane domain, three low complexity regions and one GSDH domain. Five SNPs in IR26 caused amino acid residue change in the coding region compared with Jiucaiqing, including SNP3 and SNP6 located in GSDH domain and the third low complexity region respectively. This change may result in higher seed vigour of IR26 than Jiucaiqing.

It is well-known that ABA is a sesquiterpenoid hormone that plays central roles in seed maturation, germination and stress responsiveness (Finkelstein *et al.*, 2002). In our study, the ABA content in germinating seeds of *Oshipl1* mutants and NIL-*qsv3* line was significantly higher than that of IR26 plants (Figure 5a), indicating that the decrease in seed vigour of *Oshipl1* mutants and NIL-*qsv3* line might be due to the increased level of endogenous ABA in seeds. We hypothesized that the seed germination controlled by *OsHIPL1* is involved in ABA metabolism. It is also confirmed by the reduced transcript abundance of *OsABA8ox3* and increased transcript levels of the *OsZEP* and *OsNCED4* in NIL-*qsv3* line and *Oshipl1* mutants compared with IR26 (Figure 5b,c). Transcription factors, ABI3, ABI4 and ABI5, as positive regulators in ABA signalling, contributed to delayed seed germination in plants (Albertos *et al.*, 2015; Nambara *et al.*, 1995; Nonogaki, 2019; Shu *et al.*, 2013; Zhang *et al.*, 2005). The higher transcript levels of *OsABI3*, *OsABI4* and *OsABI5* were observed in germinating seeds of NIL-*qsv3* line and *Oshipl1* mutants compared with IR26 in this study (Figure 5d–f). It indicates that *OsHIPL1* modulated the expression of *OsABI3*, *OsABI4* and *OsABI5*. Previous studies show that

increased expression of *OsABI3*, *OsABI4* and *OsABI5* reduces seed germination and seedling establishment (He *et al.*, 2020; Nonogaki, 2019). These results indicate that the higher endogenous ABA and higher expressions of *OsABIs* in germinating seeds of *Oshipl1* mutants and NIL-*qsv3* line lead to the decreases in seed vigour in mutants and NIL-*qsv3* line. We also measured IAA content of *oship1a*, *oship1b* and IR26 in germinated seeds, while no obvious differences were identified between *oship11* mutants and IR26 (Figure S15). It hints that function of *OsHIPL1* on seed vigour might be different from that of *OsAGLU*, which regulates seed vigour through mediating crosstalk between IAA and ABA reported by He *et al.* (2020).

Aquaporins, belonging to the highly conserved major intrinsic protein (MIP) family, play an essential role in plant water transport (Footitt *et al.*, 2019; Liu *et al.*, 2007, 2013; Roche and Törnroth-Horsefield, 2017). The co-expression of aquaporins ZmPIP1;2 and ZmPIP2;1 in *X. laevis* oocytes increased the cell osmotic water permeability coefficient (P_f) (Fetter *et al.*, 2004). Zelazny *et al.* (2007) demonstrated that interactions between ZmPIP1s and ZmPIP2s occurred in maize mesophyll protoplasts, and the PIP1–PIP2 interaction induced the relocation of ZmPIP1s to the plasma membrane. Liu *et al.* (2013) reported that co-expression of *OsPIP2;1* with *OsPIP1;1* could help *OsPIP1;1* incorporating into plasma membrane and significantly increasing its water permeability. Our results showed that *OsHIPL1* could interact with *OsPIP1;1* and co-locate in the plasma membrane. It suggested that *OsHIPL1*, like *OsPIP2;1*, might make *OsPIP1;1* incorporating into plasma membrane and significantly increase water uptake for seed germination. The molecular mechanism of *OsHIPL1* interacting with *OsPIP1;1* warrants further investigation in the future.

As previously reported, the moderate expression of *OsPIP1;1* increased seed germination of rice (Liu *et al.*, 2013). Similar results were observed in this study, the alteration of expression levels of *OsPIP1;1* was observed in *Oshipl1* mutants, NIL-*qsv3* and COM lines during seed germination, while not in OE lines (Figure 6g). It indicates that the excess *OsHIPL1* proteins could not enhance the expression levels of *OsPIP1;1* during seed germination. The expression of *OsHIPL1* was increased under ABA treatments during seed germination (Figure S9), while the expression of *OsPIP1;1* was decreased (Figure 6h). We proposed that under normal condition (without ABA treatment), *OsHIPL1* could up-regulate *OsPIP1;1* expression, but under ABA treatment, the excess expression of *OsHIPL1* induced could not synchronously affect the *OsPIP1;1* expression. Guo *et al.* (2006) reported that the *OsPIP1;1* expression was significantly inhibited by ABA treatment in roots in the seedling stage of rice, similar to our results.

ABA can influence activity of aquaporins at different levels by either changing the expression of aquaporin genes or post-transcriptional modifications (Jang *et al.*, 2004; Mariaux *et al.*, 1998; Suga *et al.*, 2002; Zhu *et al.*, 2005). ABA-induced dephosphorylation of aquaporins leads to reduced water flux (Kline *et al.*, 2010). ABA-dependent changes in dormancy and germination also result from shifting water potential thresholds for radicle emergence (Ni and Bradford, 1992). In *Arabidopsis*, the expression of *CYP707A2*, which encodes an ABA 8'-hydroxylase, rapidly increases after seed imbibition and plays a key role in inactivating ABA during germination (Kushiro *et al.*, 2004). We thus speculated that the crosstalk of ABA metabolism and seed imbibition might influence seed vigour. In our study, the *Oshipl1*

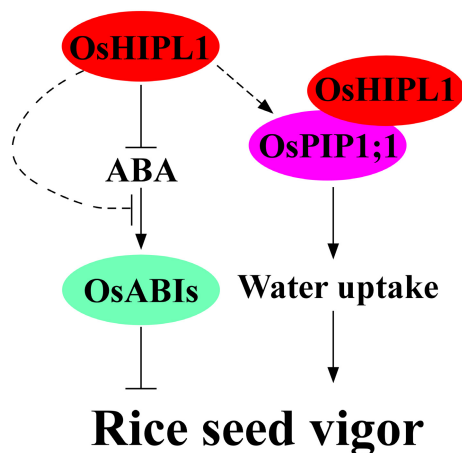


Figure 9 Proposed model for the role of *OsHIPL1* in seed vigour in rice. This model shows that *OsHIPL1* might reduce the endogenous ABA contents in germinating seeds, which could decrease the expression levels of the ABA signalling-related genes *ABI3/4/5*, and then improve rice seed vigour. In addition, *OsHIPL1* might affect the expression of *OsPIP1;1*, and the complex of *OsHIPL1* with *OsPIP1;1* could regulate water uptake to increase seed vigour.

mutants have lower imbibition rate that might cause lower ABA degradation in germinating seeds, but the molecular mechanism needs to be further investigated.

Summary, we clarified the function of hedgehog-interacting protein-like 1 protein gene *OsHIPL1* in plants. Although it is unknown whether *OsHIPL1* has similar pathway as hedgehog signalling in plants as in humans, there are two possible pathways by which *OsHIPL1* regulates seed vigour in rice (Figure 9). On the one hand, *OsHIPL1* contributed to seed germination and seedling establishment involved in modulating ABA levels and ABA signalling in germinating seeds in rice. On the other hand, *OsHIPL1* interacted with the *OsPIP1;1*, and regulated the water uptake to improve rice seed vigour. However, it is worthy to further study how *OsHIPL1* influences the expressions of *OsABIs*, and what other factors in the interaction of *OsHIPL1* and *OsPIP1;1* regulate the germination of seeds. Our studies provide a novel gene *OsHIPL1* and its information on the molecular mechanisms of seed vigour. Meanwhile, the superior haplotype Hap1 and its linkage molecular marker SNP3 of *OsHIPL1* were identified, which would facilitate improvement in seed vigour in rice breeding programme and be beneficial to production of rice direct seeding.

Materials and methods

Plant materials and growth conditions

Japonica Jiucaiqing and *indica* IR26, and 62 CSSLs developed by introgressing chromosome segments of Jiucaiqing into IR26 (Cheng et al., 2016, Tables S1 and S2), were used for QTL mapping. A residual heterozygous line CSSL10 (BC₆F₂) and its selfing population were used for the confirmation of the major *qSV3*. One heterozygous line (BC₆F₃) between markers HY27 and HY44 from the selfing segregation population of line CSSL10 was selected to develop the genetic population I (BC₆F₄, 5000 individuals) and population II (BC₆F₅, 992 individuals) by selfing for fine mapping of the *qSV3* locus. A homozygous line containing the allele (*qsv3*) from Jiucaiqing between markers HY42 and HY43 was selected for the development of NIL-*qsv3*. In

total, 192 accessions from the rice diversity panel (Eizenga et al., 2014) were used for haplotype analyses of *qSV3* locus (Table S7). All plants were grown in an experimental field at Nanjing Agricultural University, Nanjing, Jiangsu. All seeds were harvested at their maturity stage and dried at 42 °C for 7 days to break seed dormancy.

Evaluation of seed vigour

Seed germination was conducted as previously described by Wang et al. (2010). Thirty seeds of each genotype were imbibed in Petri dishes (diameter 9 cm) with 10 mL distilled water at 30 ± 1 °C for 7 days. Seeds were also treated with 10 mL of 20% PEG6000 (polyethylene glycol with an average molecular weight of 6000 Da), 300 mM mannitol and 20 mL of 200 mM NaCl at 30 ± 1 °C for 11 days, respectively, and with 10 mL of distilled water at 15 ± 1 °C for 11 days. As to ABA treatments, distilled water was replaced with the solution containing 0, 1 and 3 μM of ABA respectively. The number of germinated seeds was observed daily. Germination was defined as the emergence of the radicle through the hull by ≥2 mm. Seedlings were considered to have developed when the root length reached the seed length and the shoot length reached half of the seed length (Xu et al., 2017). Three replications were performed. GP, SP and GI were calculated as follows: GP = (total germinated seeds/30) × 100%, SP = (total seedlings/30) × 100% and GI = $\sum(Gt/t)$, where *Gt* is the number of germinated seeds on Day *t* (Wang et al., 2010).

Map-based cloning

The GP, GI and SP of the individual among CSSLs were used by SMA for QTL mapping, and the confirmation of major *qSV3* was conducted by ICIM (Li et al., 2008). Genomic DNA of seedlings from the population I and population II was extracted using the cetyltrimethylammonium bromide (CTAB) method to screen recombinants for fine mapping (Murray and Thompson, 1980). Markers used for QTL mapping are listed in Table S7. The candidate gene was predicted using the data at <http://rice.plantbiology.msu.edu/cgi-bin/gbrowse>. The cDNA sequences of the predicted gene were amplified from Jiucaiqing and IR26 using Phanta Super-Fidelity DNA polymerase (Vazyme Biotech Co., Ltd, Nanjing, Jiangsu, China).

Plasmid construction and plant transformation

For generating *OsHIPL1*-overexpressing lines, the full-length coding sequence of *OsHIPL1* was cloned into PBWA(V)HS, driven by 35S promoter and then transformed into *japonica* Zhonghua11 (ZH11) by *Agrobacterium tumefaciens*-mediated transformation (Hiei et al., 1994). The *Oshipl1* mutants (IR26 background) were generated by CRISPR-Cas9 system (Xing et al., 2014). To produce the complementation construct PBWA(V)HS-*OsHIPL1*_{pro-c} *OsHIPL1*, the full-length CDS of *OsHIPL1* (2079 bp) was cloned by RT-qPCR amplification. The CDS containing the entire *OsHIPL1* coding region was inserted into the modified vector PBWA(V)HS, and then the *OsPHF1* promoter was amplified from IR26 genomics DNA and inserted before *OsHIPL1*-coding region to generate the vector PBWA(V)HS-*OsHIPL1*_{pro-c} *OsHIPL1*. The vectors were introduced into NIL-*qsv3* line using the *Agrobacterium*-mediated transformation method. All DNA constructs were confirmed by sequencing, and all transgenic plants were identified by the RT-qPCR and hygromycin gene amplification. Specific primers were designed to confirm the mutation positions in each CRISPR/Cas9-positive transgenic line. All primers are listed in Table S8.

Expression analysis

Total RNA was extracted from the developing grains (0, 7, 14, 28 and 35 days after flowering; DAF), germinating seeds (0, 6, 12, 24, 30, 36, 48, 54, 60 and 72 h imbibition) and different tissues (root, stem, leaf, sheath, node and spike) of IR26 using the HP Plant RNA kit (Omega, Atlanta), according to the manufacturer's instructions. First-strand cDNA was synthesized with random oligonucleotides using the HiScriptII Reverse Transcriptase system (Vazyme Biotech Co., Ltd.). The RT-qPCR was performed on a Roche Light Cycler 480 system using SYBR Green Mix. The *Actin* gene was used as the internal control for normalization. Primers used for expression analysis are listed in Table S8. Three biological replicates were made.

Subcellular localization

The open reading frame of *OsHIPL1* (without the stop codon) was amplified and inserted into the pCambia1300s-GFP vector driven by the CaMV 35S promoter and the PAN580-GFP vector driven by the CaMV 35S promoter according to the manufacturer's instructions (Vazyme, Nanjing, China). Then, the construct was introduced into *Agrobacterium tumefaciens* strain EH105 and infiltrated into rice protoplasts and *N. benthamiana* leaves (Chen *et al.*, 2008). Fluorescence signals were observed using a LSM 710 confocal microscope (Zeiss, Oberkochen, Germany).

Phylogenetic analysis

The entire amino acid sequences of *OsHIPL1* were used as the query to search for the homologous proteins in the NCBI website (<https://blast.ncbi.nlm.nih.gov/Blast.cgi>) and GBI website (<https://phytozome.jgi.doe.gov>). All HIPL1 proteins were clustered using ClustalX, and the phylogenetic tree was generated by MEGA6 based on the neighbour-joining method and bootstrap analysis (1000 replicates).

Hormone quantification

The extraction and quantification of endogenous ABA were conducted according to the manufacturer's instructions (Wuhan Metware Biotechnology Co., Ltd., Wuhan, China). The ABA content was quantified by LC-MS/MS system as described by He *et al.* (2020). Three biological replicates were conducted.

RNA-seq analysis

The IR26 and NIL-*qsv3* seeds were grown on media for 12 h, and then the materials were collected. Three biological replicates were prepared for each sample. Total RNA was extracted using HP Plant RNA kit (Omega, Atlanta, GA) according to the manufacturer's instructions and then sequenced (PERSONAL, Nanjing, China). Clean reads were mapped to the *japonica* rice Nipponbare reference genome after screening and trimming. Genes with *P*-value < 0.05 and fold change ≥ 2 were identified as reliable differentially expressed genes (DEGs). Multiple testing was corrected via false discovery rate estimation and *q*-values below 0.05 were considered to indicate differential expression. Twelve genes were randomly selected for the confirmation of RNA-seq by the RT-qPCR and their primers are listed in Table S8.

Y2H screening and confirmation

DUAL Membrane Pairwise Interaction kit (Dualsystems Biotech) and cDNA library of seeds were used for the Y2H assays. The full-length CDS of *OsHIPL1* was fused to PBT3-N to construct the bait vector, which was transformed into the yeast strain NMY51.

Yeast screening was performed as described in the manufacturer's protocol (Clontech Yeast Protocols Handbook). To confirm protein-protein interaction in yeast, the full-length CDS of *OsPIP1;1* was cloned into the pPR3-N vector to generate *NubG-OsPIP1;1*. The recombinant plasmid pairs were co-transformed into the yeast strain NMY51. The transfected yeast cells were plated on SD/-Leu/-Trp medium and SD/-Ade/-His/-Leu/-Trp medium and cultured at 28 °C for 4 days. The primers and restriction enzyme sites were used to amplify sequences and generate vectors. The relevant primers are listed in Table S8.

BiFC assay

The *OsHIPL1* and *OsPIP1;1* cDNA fragments were cloned into p2YN and p2YC to form the nYFP protein and cYFP protein constructs respectively. The plasmids were then transformed into *A. tumefaciens* strain EH105 and all constructs were verified by DNA sequencing. For the transient expression assay, these constructs were co-infiltrated with the p19 strain into 5-week-old *N. benthamiana* leaves. YFP fluorescence was excited at 515 nm by a Zeiss LSM780 confocal scanning microscope in dark for 48 hours after infiltration. Primers used to generate the constructs are listed in Table S8.

Luciferase (LUC) assays

The pCAMBIA1300-cLUC-*OsHIPL1* and pCAMBIA1300-nLUC-*OsPIP1;1* plasmids were generated by CDS of *OsHIPL1* and *OsPIP1;1*. The LUC assays were performed as previously described with some modifications (Chen *et al.*, 2008). Different recombinant plasmids including nLUC-*OsPIP1;1* and cLUC-*OsHIPL1* with the control vector were introduced into *Agrobacterium* strain EH105. *Agrobacterium* cultures were resuspended overnight with infiltration buffer (10 mM MgCl₂, 0.1 mM acetosyringone and 10 mM MES). Different experiment and control group *agrobacterium* suspension were mixed and co-infiltrated into 5- to 6-week-old *Nicotiana benthamiana* leaves by using a needleless syringe, then weak light growth. Luciferin (1 mM) was sprayed onto the leaves, and the plants were kept in the dark for 2–5 min. LUC images were captured using a cooled CCD imaging apparatus (Chen *et al.*, 2008). The primers were listed in Table S8.

Haplotype analysis

To determine the haplotypes of the *OsHIPL1*, the 700 000 SNP markers of rice accessions at <https://ricediversity.org/data/index.cfm> (McCouch *et al.*, 2016) were used. Four SNPs in the full-length coding region of *OsHIPL1* were located according to the Rice Genome Annotation Project MSU7 database (Rice Genome Browser: <http://rice.plantbiology.msu.edu>). Seed germination was conducted using 192 accessions under H₂O condition for 7 days (Table S7). The haplotypes represented at least 10 investigated accessions that were previously used for a comparative analysis of phenotype (Dong *et al.*, 2016).

Direct sowing rice assay

Forty healthy seeds of IR26, NIL-*qsv3*, ZH11, *Oship1* mutants, complementation and overexpression lines were sowed 1 cm deep in soil in the same plot in an incubator with a 14 h : 10 h, light : dark cycle at 30 °C : 25 °C with 100% relative humidity. Similarly, wild-type and transgenic lines were sowed 1 cm deep in rice fields with water saturation of 100% for 22 days in June 2021, during which the average high and low temperature ranged from 22 to 29 °C. The SP on the 5th day, root length, shoot length and basal shoot diameter on the 10th day were

investigated and calculated. Three biological replicates were made.

Data analysis

Experimental data were analysed using the SAS software (Cary, NC), and significant differences among samples were compared using Student's *t*-test or Fisher's least significant difference (LSD) test at the 5%, 1% and 0.1% levels of probability.

Acknowledgements

We thank Dr. Jian Hua at Cornell University and Nanjing Agricultural University for seeds and Dr. Susan McCouch at Cornell University for seeds of the Rice Diversity Panel.

Conflicts of interest

The authors declare no conflict of interest.

Author contributions

Ying He, Jinping Cheng and Hongsheng Zhang planned the research, analysed the data and drafted the manuscript. Ying He performed all important experiments. Shanshan Chen, Kexin Liu, Yongji Chen, Yanhao Cheng, Peng zeng, Peiwen Zhu and Ting Xie performed part of the seed germination experiments. Sunlu Chen provided reliable experimental advice.

Funding

This work was supported by the Hainan Yazhou Bay Seed Laboratory (Project of B21HJ1002), the Natural Science Foundation of Jiangsu Province (Grant No. SBK2020020068) and the National Natural Science Foundation of China (Grant No. 32172037, 32000377 and 31771757).

References

- Abe, A., Takagi, H., Fujibe, T., Aya, K., Kojima, M., Sakakibara, H., Uemura, A. et al. (2012) *OsGA20ox1*, a candidate gene for a major QTL controlling seedling vigor in rice. *Theor. Appl. Genet.* **125**, 647–657.
- Albertos, P., Romero-Puertas, M.C., Tatematsu, K., Mateos, I., Sanchez-Vicente, I., Nambara, E. and Lorenzo, O. (2015) S-nitrosylation triggers ABI5 degradation to promote seed germination and seedling growth. *Nat. Commun.* **6**, 8669.
- Aravani, D., Morris, G.E., Jones, P.D., Tattersall, H.K., Karamanavi, E., Kaiser, M.A., Kostogryz, R.B. et al. (2019) *HHLPL1*, a gene at the 14q32 coronary artery disease locus, positively regulates hedgehog signaling and promotes atherosclerosis. *Circulation*, **140**, 500–513.
- Arraf, A.A., Yelin, R., Reshef, I., Jadon, J., Abboud, M., Zaher, M., Schneider, J. et al. (2020) Hedgehog signaling regulates epithelial morphogenesis to position the ventral embryonic midline. *Dev. Cell*, **53**, 589–602.
- Bailly, C., El-Maarouf-Bouteau, H. and Corbineau, F. (2008) From intracellular signaling networks to cell death: the dual role of reactive oxygen species in seed physiology. *C R Biol.* **331**, 806–814.
- Bewley, J.D. (1997) Seed germination and dormancy. *Plant Cell*, **9**, 1055–1066.
- Bewley, J.D., Bradford, K., Hilhorst, H. and Nonogaki, H. (2013) *Seeds: Physiology of Development, Germination and Dormancy*, 3rd ed. Heidelberg: Springer.
- Borner, G.H., Lilley, K.S., Stevens, T.J. and Dupree, P. (2003) Identification of glycosylphosphatidylinositol-anchored proteins in *Arabidopsis*. A proteomic and genomic analysis. *Plant Physiol.* **132**, 568–577.
- Borner, G.H., Sherrier, D.J., Stevens, T.J., Arkin, I.T. and Dupree, P. (2002) Prediction of glycosylphosphatidylinositol-anchored proteins in *Arabidopsis*. A genomic analysis. *Plant Physiol.* **129**, 486–499.
- Chen, H.M., Zou, Y., Shang, Y.L., Lin, H.Q., Wang, Y.J., Cai, R., Tang, X.Y. et al. (2008) Firefly luciferase complementation imaging assay for protein-protein interactions in plants. *Plant Physiol.* **146**, 368–376.
- Chen, K., Li, G.J., Bressan, R.A., Song, C.P., Zhu, J.K. and Zhao, Y. (2020) Abscisic acid dynamics, signaling, and functions in plants. *J. Integr. Plant Biol.* **62**, 25–54.
- Cheng, J.P., He, Y.Q., Zhan, C.F., Yang, B., Xu, E.S., Zhang, H.S. and Wang, Z.F. (2016) Identification and characterization of quantitative trait loci for shattering in rice Landrace Jiuciaiqing from Taihu Lake Valley, China. *Plant Genome*, **9**, 1–9.
- Chuang, P.T., Kawcak, T. and McMahon, A.P. (2003) Feedback control of mammalian Hedgehog signaling by the Hedgehog-binding protein, Hip1, modulates Fgf signaling during branching morphogenesis of the lung. *Genes Dev.* **17**, 342–347.
- Chuang, P.T. and McMahon, A.P. (1999) Vertebrate Hedgehog signalling modulated by induction of a Hedgehog-binding protein. *Nature*, **397**, 617–621.
- Cutler, S.R., Rodriguez, P.L., Finkelstein, R.R. and Abrams, S.R. (2010) Abscisic acid: emergence of a core signaling network. *Annu. Rev. Plant Biol.* **61**, 651–679.
- Debeaujon, I. and Koornneef, M. (2000) Gibberellin requirement for *Arabidopsis* seed germination is determined both by testa characteristics and embryonic abscisic acid. *Plant Physiol.* **122**, 415–424.
- Ding, Z.J., Yan, J.Y., Li, G.X., Wu, Z.C., Zhang, S.Q. and Zheng, S.J. (2014) WRKY41 controls *Arabidopsis* seed dormancy via direct regulation of *ABI3* transcript levels not downstream of ABA. *Plant J.* **79**, 810–823.
- Dong, H., Zhao, H., Xie, W., Han, Z., Li, G., Yao, W., Bai, X. et al. (2016) A novel tiller angle gene, *TAC3*, together with *TAC1* and *D2* largely determine the natural variation of tiller angle in rice cultivars. *PLoS Genet.* **12**, e1006412.
- Eiji, N., Masanori, O., Kiyoshi, T., Ryoichi, Y., Mitsunori, S. and Yuji, K. (2010) Abscisic acid and the control of seed dormancy and germination. *Seed Sci. Res.* **20**, 55–67.
- Eizenga, G.C., Ali, M.L., Bryant, R.J., Yeater, K.M., McClung, A.M. and McCouch, S.R. (2014) Registration of the Rice Diversity Panel 1 for genome wide association studies. *J. Plant Reg.* **8**, 109–116.
- El-Maarouf-Bouteau, H. and Bailly, C. (2008) Oxidative signaling in seed germination and dormancy. *Plant Signal Behav.* **3**, 175–182.
- Fetter, K., Van Wilder, V., Moshelion, M. and Chaumont, F. (2004) Interactions between plasma membrane aquaporins modulate their water channel activity. *Plant Cell*, **16**, 215–228.
- Finkelstein, R.R., Gampala, S.S. and Rock, C.D. (2002) Abscisic acid signaling in seeds and seedlings. *Plant Cell*, **14**(Suppl), S15–45.
- Finkelstein, R.R. and Lynch, T.J. (2000) The *Arabidopsis* abscisic acid response gene *ABI5* encodes a basic leucine zipper transcription factor. *Plant Cell*, **12**, 599–609.
- Finkelstein, R., Reeves, W., Ariizumi, T. and Steber, C. (2008) Molecular aspects of seed dormancy. *Annu. Rev. Plant Biol.* **59**, 387–415.
- Foolad, M.R., Subbiah, P. and Zhang, L. (2007) Common QTL affect the rate of tomato seed germination under different stress and non stress conditions. *Int. J. Plant Genomics*, **2007**, 97386.
- Footitt, S., Clewes, R., Feeney, M., Finch-Savage, W.E. and Frigerio, L. (2019) Aquaporins influence seed dormancy and germination in response to stress. *Plant Cell Environ.* **42**, 2325–2339.
- Fujino, K., Sekiguchi, H., Sato, T., Kiuchi, H., Nonoue, Y., Takeuchi, Y., Ando, T. et al. (2004) Mapping of quantitative trait loci controlling low-temperature germinability in rice (*Oryza sativa* L.). *Theor. Appl. Genet.* **108**, 794–799.
- Fujino, K., Sekiguchi, H., Matsuda, Y., Sugimoto, K., Ono, K. and Yano, M. (2008) Molecular identification of a major quantitative trait locus, *qLTG3-1*, controlling low-temperature germinability in rice. *Proc. Natl Acad. Sci. USA*, **105**, 12623–12628.
- Gommers, C.M.M. and Monte, E. (2018) Seedling establishment: a dimmer switch-regulated process between dark and light signaling. *Plant Physiol.* **176**, 1061–1074.
- Guo, L., Wang, Z.Y., Lin, H., Cui, W.E., Chen, J., Liu, M.H., Chen, Z.L. et al. (2006) Expression and functional analysis of the rice plasma-membrane intrinsic protein gene family. *Cell Res.* **16**, 277–286.
- Hammerschmidt, M., Brook, A. and McMahon, A.P. (1997) The world according to hedgehog. *Trends Genet.* **13**, 14–21.

- He, D. and Yang, P.F. (2013) Proteomics of rice seed germination. *Front. Plant Sci.* **4**, 246.
- He, Y.Q., Yang, B., He, Y., Zhan, C.F., Cheng, Y.H., Zhang, J.H., Zhang, H.S. et al. (2019) A quantitative trait locus, *qSE3*, promotes seed germination and seedling establishment under salinity stress in rice. *Plant J.* **97**, 1089–1104.
- He, Y.Q., Zhao, J., Yang, B., Sun, S., Peng, L.L. and Wang, Z.F. (2020) Indole-3-acetate beta-glucosyltransferase *OsiAGLU* regulates seed vigour through mediating crosstalk between auxin and abscisic acid in rice. *Plant Biotechnol. J.* **18**, 1933–1945.
- Hiei, Y., Ohta, S., Komari, T. and Kumashiro, T. (1994) Efficient transformation of rice (*Oryza sativa* L.) mediated by *Agrobacterium* and sequence analysis of the boundaries of the T-DNA. *Plant J.* **6**, 271–282.
- Jang, J.Y., Kim, D.G., Kim, Y.O., Kim, J.S. and Kang, H. (2004) An expression analysis of a gene family encoding plasma membrane aquaporins in response to abiotic stresses in *Arabidopsis thaliana*. *Plant Mol. Biol.* **54**, 713–725.
- Jiang, J. (2021) Hedgehog signaling mechanism and role in cancer. *Sem. Cancer Biol.* S1044-579X(21)00104-8.
- Jiang, N., Shi, S., Shi, H., Khanzada, H., Wassan, G.M., Zhu, C., Peng, X. et al. (2017) Mapping QTL for seed germinability under low temperature using a new high-density genetic map of rice. *Front. Plant Sci.* **8**, 1223.
- Jiang, W., Lee, J., Jin, Y.M., Qiao, Y., Piao, R., Jang, S.M., Woo, M.O. et al. (2011) Identification of QTLs for seed germination capability after various storage periods using two RIL populations in rice. *Mol. Cells*, **31**, 385–392.
- Kang, J.Y., Choi, H.I., Im, M.Y. and Kim, S.Y. (2002) *Arabidopsis* basic leucine zipper proteins that mediate stress responsive abscisic acid signaling. *Plant Cell*, **14**, 343–357.
- Katoh, Y. and Katoh, M. (2006) Comparative genomics on HHIP family orthologs. *Int. J. Mol. Med.* **17**, 391–395.
- Kline, K.G., Barrett-Wilt, G.A. and Sussman, M.R. (2010) In planta changes in protein phosphorylation induced by the plant hormone abscisic acid. *Proc. Natl Acad. Sci. USA*, **107**, 15986–15991.
- Kumar, V. and Ladha, J.K. (2011) Direct seeding of rice: recent developments and future research needs. *Adv. Agron.* **111**, 297–413.
- Kushiro, T., Okamoto, M., Nakabayashi, K., Yamagishi, K., Kitamura, S., Asami, T., Hirai, N. et al. (2004) The *Arabidopsis* cytochrome P450 CYP707A encodes ABA 8'-hydroxylases: key enzymes in ABA catabolism. *EMBO J.* **23**, 1647–1656.
- Li, H.H., Ribaut, J.M., Li, Z.L. and Wang, J.K. (2008) Inclusive composite interval mapping (ICIM) for digenic epistasis of quantitative traits in biparental populations. *Theor. Appl. Genet.* **116**, 243–260.
- Li, Z.H., Zhang, J., Liu, Y.L., Zhao, J.H., Fu, J.J., Ren, X.L., Wang, G.Y. et al. (2016) Exogenous auxin regulates multi-metabolic network and embryo development, controlling seed secondary dormancy and germination in *Nicotiana tabacum* L. *BMC Plant Biol.* **16**, 41.
- Liu, C.W., Fukumoto, T., Matsumoto, T., Gena, P., Frascaria, D., Kaneko, T., Katsuhara, M. et al. (2013) Aquaporin *OsPIP1;1* promotes rice salt resistance and seed germination. *Plant Physiol. Biochem.* **63**, 151–158.
- Liu, H.Y., Hussain, S., Zheng, M.M., Peng, S.B., Huang, J.L., Cui, K.H. and Nie, L.X. (2015) Dry direct-seeded rice as an alternative to transplanted-flooded rice in central China. *Agron Sustain. Dev.* **35**, 285–294.
- Liu, H.Y., Yu, X., Cui, D.Y., Sun, M.H., Sun, W.N., Tang, Z.C., Kwak, S.S. et al. (2007) The role of water channel proteins and nitric oxide signaling in rice seed germination. *Cell Res.* **17**, 638–649.
- Liu, L.F., Lai, Y.Y., Cheng, J.P., Wang, L., Du, W.L., Wang, Z.F. and Zhang, H.S. (2014) Dynamic quantitative trait locus analysis of seed vigor at three maturity stages in rice. *PLoS One*, **9**, e115732.
- Lopez-Molina, L., Mongrand, S. and Chua, N.H. (2001) A post germination developmental arrest checkpoint is mediated by abscisic acid and requires the *ABI5* transcription factor in *Arabidopsis*. *Proc. Natl Acad. Sci. USA*, **98**, 4782–4787.
- Luo, X.F., Dai, Y.J., Zheng, C., Yang, Y.Z., Chen, W., Wang, Q.C., Chandrasekaran, U. et al. (2021) The *ABI4-RbohD/VTC2* regulatory module promotes reactive oxygen species (ROS) accumulation to decrease seed germination under salinity stress. *New Phytol.* **229**, 950–962.
- Ma, Y., Szostkiewicz, I., Korte, A., Moes, D., Yang, Y., Christmann, A. and Grill, E. (2009) Regulators of PP2C phosphatase activity function as abscisic acid sensors. *Science*, **324**, 1064–1068.
- Mahender, A., Anandan, A. and Pradhan, S.K. (2015) Early seedling vigour, an imperative trait for direct-seeded rice, an overview on physio-morphological parameters and molecular markers. *Planta*, **241**, 1027–1050.
- Mariaux, J.B., Bockel, C., Salamini, F. and Bartels, D. (1998) Desiccation- and abscisic acid-responsive genes encoding major intrinsic proteins (MIPs) from the resurrection plant *Craterostigma plantagineum*. *Plant Mol. Biol.* **38**, 1089–1099.
- McCouch, S.R., Wright, M.H., Tung, C.-W., Maron, L.G., McNally, K.L., Fitzgerald, M., Singh, N. et al. (2016) Open access resources for genome-wide association mapping in rice. *Nat. Commun.* **7**, 10532.
- Murray, M.G. and Thompson, W.F. (1980) Rapid isolation of high molecular weight plant DNA. *Nucleic Acids Res.* **8**, 4321–4325.
- Nambara, E., Keith, K., McCourt, P. and Naito, S. (1995) A regulatory role for the *ABI3* gene in the establishment of embryo maturation in *Arabidopsis thaliana*. *Development*, **121**, 629–636.
- Ni, B.R. and Bradford, K.J. (1992) Quantitative models characterizing seed germination responses to abscisic acid and osmoticum. *Plant Physiol.* **98**, 1057–1068.
- Nonogaki, H. (2019) ABA responses during seed development and germination. *Adv. Bot Res.* **92**, 171–217.
- Palaniyandi, S.A., Chung, G., Kim, S.H. and Yang, S.H. (2015) Molecular cloning and characterization of the ABA-specific glucosyltransferase gene from bean (*Phaseolus vulgaris* L.). *J. Plant Physiol.* **178**, 1–9.
- Park, S.-Y., Fung, P., Nishimura, N., Jensen, D.R., Fujii, H., Zhao, Y., Lumba, S. et al. (2009) Abscisic acid inhibits type 2C protein phosphatases via the PYR/PYL family of START proteins. *Science*, **324**, 1068–1071.
- Penfield, S. (2017) Seed dormancy and germination. *Curr. Biol.* **27**, R874–R878.
- Rajjou, L., Duval, M., Gallardo, K., Catusse, J., Bally, J., Job, C. and Job, D. (2012) Seed germination and vigor. *Annu. Rev. Plant Biol.* **63**, 507–533.
- Rallis, A., Navarro, J.A., Rass, M., Hu, A., Birman, S., Schneuwly, S. and Thérond, P.P. (2020) Hedgehog signaling modulates glial proteostasis and lifespan. *Cell Rep.* **30**, 2627–2643.e5.
- Rao, A.N., Johnson, D.E., Sivaprasad, B., Ladha, J.K. and Mortimer, A.M. (2007) Weed management in direct-seeded rice. *Adv. Agron.* **93**, 153–255.
- Roche, J.V. and Törnroth-Horsefield, S. (2017) Aquaporin protein-protein interactions. *Int. J. Mol. Sci.* **18**, 2255.
- Sano, N. and Marion-Poll, A. (2021) ABA metabolism and homeostasis in seed dormancy and germination. *Int. J. Mol. Sci.* **22**, 5069.
- Seiler, C., Harshavardhan, V.T., Rajesh, K., Reddy, P.S., Strickert, M., Rolletschek, H., Scholz, U. et al. (2011) ABA biosynthesis and degradation contributing to ABA homeostasis during barley seed development under control and terminal drought-stress conditions. *J. Exp. Bot.* **62**, 2615–2632.
- Sherrier, D.J., Prime, T.A. and Dupree, P. (1999) Glycosylphosphatidylinositol-anchored cell-surface proteins from *Arabidopsis*. *Electrophoresis*, **20**, 2027–2035.
- Shu, K., Liu, X.D., Xie, Q. and He, Z.H. (2016) Two faces of one seed: hormonal regulation of dormancy and germination. *Mol. Plant*, **9**, 34–45.
- Shu, K., Zhang, H.W., Wang, S.F., Chen, M.L., Wu, Y.R., Tang, S.Y., Liu, C.Y. et al. (2013) *ABI4* regulates primary seed dormancy by regulating the biogenesis of abscisic acid and gibberellins in *Arabidopsis*. *PLoS Genet.* **9**, e1003577.
- Söderman, E.M., Brocard, I.M., Lynch, T.J. and Finkelstein, R.R. (2000) Regulation and function of the *Arabidopsis* ABA-insensitive 4 gene in seed and abscisic acid response signaling networks. *Plant Physiol.* **124**, 1752–1765.
- Song, J.W., Shang, L.L., Wang, X., Xing, Y.L., Xu, W., Zhang, Y.Y., Wang, T.T. et al. (2021) MAPK11 regulates seed germination and ABA signaling in tomato by phosphorylating SnRKs. *J. Exp. Bot.* **72**, 1677–1690.
- Suga, S., Komatsu, S. and Maeshima, M. (2002) Aquaporin isoforms responsive to salt and water stresses and phytohormones in radish seedlings. *Plant Cell Physiol.* **43**, 1229–1237.
- Tabin, C.J. and McMahon, A.P. (1997) Recent advances in Hedgehog signaling. *Trends Cell Biol.* **7**, 442–446.
- Vander Willigen, C., Postaire, O., Tournaire-Roux, C., Boursiac, Y. and Maurel, C. (2006) Expression and inhibition of aquaporins in germinating *Arabidopsis* seeds. *Plant Cell Physiol.* **47**, 1241–1250.
- Wang, Z.F., Wang, J.F., Bao, Y.M., Wang, F.H. and Zhang, H.S. (2010) Quantitative trait loci analysis for rice seed vigor during the germination stage. *J. Zhejiang Univ. Sci. B*, **11**, 958–964.

- Xie, L.X., Tan, Z.W., Zhou, Y., Xu, R.B., Feng, L.B., Xing, Y.Z. and Qi, X.Q. (2014) Identification and fine mapping of quantitative trait loci for seed vigor in germination and seedling establishment in rice. *J. Integr. Plant Biol.* **56**, 749–759.
- Xing, H.L., Dong, L., Wang, Z.P., Zhang, H.Y., Han, C.Y., Liu, B., Wang, X.C. et al. (2014) A CRISPR/Cas9 toolkit for multiplex genome editing in plants. *BMC Plant Biol.* **14**, 327.
- Xu, E.S., Chen, M.M., He, H.Y., Zhan, C.F., Cheng, Y.H., Zhang, H.S. and Wang, Z.F. (2017) Proteomic Analysis reveals proteins involved in seed imbibition under salt stress in rice. *Front. Plant Sci.* **7**, 2006.
- Zelazny, E., Borst, J.W., Muylaert, M., Batoko, H., Hemminga, M.A. and Chaumont, F. (2007) FRET imaging in living maize cells reveals that plasma membrane aquaporins interact to regulate their subcellular localization. *Proc. Natl Acad. Sci. USA*, **104**, 12359–12364.
- Zeng, P., Zhu, P.W., Qian, L.F., Qian, X.M., Mi, Y.X., Lin, Z.F., Dong, S.N. et al. (2021) Identification and fine mapping of *qGR6.2*, a novel locus controlling rice seed germination under salt stress. *BMC Plant Biol.* **21**, 36.
- Zhang, X., Garreton, V. and Chua, N.H. (2005) The AIP2 E3 ligase acts as a novel negative regulator of ABA signaling by promoting ABI3 degradation. *Genes Dev.* **19**, 1532–1543.
- Zhu, C., Schraut, D., Hartung, W. and Schäffner, A.R. (2005) Differential responses of maize MIP genes to salt stress and ABA. *J. Exp. Bot.* **56**, 2971–2981.

Supporting information

Additional supporting information may be found online in the Supporting Information section at the end of the article.

- Figure S1** Comparison of seed germination and seedling establishment between JCQ and IR26 under normal condition.
- Figure S2** QTLs analysis of seed germination traits among F₂ population under normal condition.
- Figure S3** Comparison of coding sequences in ORF2 between IR26 and Jiucaiqing.
- Figure S4** Comparison of seed vigour between NIL-*qsv3* and IR26 under normal condition.
- Figure S5** Comparisons of the *OsHIPL1* transcript levels between transgenic lines (OE1, OE2, COM-1 and COM-2) and wild type (NIL-*qsv3* and ZH11).
- Figure S6** The confirmation of differential expression genes (DEGs) between IR26 and NIL-*qsv3* in 12h imbibed seeds via the RT-qPCR approach in rice.

Figure S7 GO enrichment analysis for differentially expressed genes (DEGs) in IR26 compared to NIL-*qsv3*.

Figure S8 Rice *OsHIPL1* altering expressions of genes involved in ABA signalling during seed germination.

Figure S9 Transcription levels of *OsHIPL1* response to ABA treatments in germinating seeds conducted using the RT-qPCR approach.

Figure S10 Comparison of seedling establishment and seedling growth between wild-type and the transgenic lines when seeds are directly sown in outdoor field soil.

Figure S11 Comparison of agronomic traits among IR26, *Oshipl1* mutants, NIL-*qsv3* and COM lines.

Figure S12 Comparison of seed germination percentage and seedling percentage between NIL-*qsv3* and IR26 under low temperature (A–C), salinity (D–F), PEG (G–I) and mannitol (J–L) stresses.

Figure S13 Comparison of seed germination percentage and seedling percentage of the transgenic lines of *OsHIPL1* under salinity (A–D) and PEG (E–H) stresses.

Figure S14 Phylogenetic relationships of *OsHIPL1* among *Oryza sativa*, Maize, Sorghum, *Setaria italica*, *Setaria viridis*, *Brachypodium*, *Brachypodium stacei*, *Arabidopsis*, *Prunus persica* and *Glycine max*.

Figure S15 The contents of IAA in germinated seeds of *Oshipl1* mutants and IR26.

Table S1 The information of phenotype of seed vigour of the CSSLs and parents.

Table S2 The information of genotype of seed vigour of the CSSLs and parents.

Table S3 The information QTLs of seed vigour identified by single marker mapping based on the CSSL population.

Table S4 Differential expression genes (DEGs) between IR26 and NIL-*qsv3* in 12h imbibed seeds in rice.

Table S5 DEGs involved in hormone metabolism between IR26 and NIL-*qsv3* in 12h imbibed seeds in rice.

Table S6 Identification of putative *OsHIPL1*-interacting proteins using yeast two-hybrid screening.

Table S7 Information of the 192 accessions used for haplotype analyses in rice.

Table S8 The primer pairs used in this study.